AGU PUBLICATIONS

Water Resources Research

RESEARCH ARTICLE
10.1002/2013WR014588

Key Points:
- Discrete groundwater discharge provides critical summer habitat for salmonids
- Climate change may impact temperature/magnitude of aquifer discharge to rivers
- These climate impacts are evaluated by linking surface and subsurface models

Supporting Information:
- Read me
- Text files 1 and 2
- Figures S1–S4

Correspondence to:
B. L. Kurylyk,
barret.kurylyk@unb.ca

Citation:
Kurylyk, B. L., K. T. B. MacQuarrie, and C. I. Voss (2014), Climate change impacts on the temperature and magnitude of groundwater discharge from shallow, unconfined aquifers, *Water Resour. Res.*, *50*, 3253–3274, doi:10.1002/2013WR014588.

Received 15 AUG 2013
Accepted 21 MAR 2014
Accepted article online 27 MAR 2014
Published online 15 APR 2014

Climate change impacts on the temperature and magnitude of groundwater discharge from shallow, unconfined aquifers

Barret L. Kurylyk[1], Kerry T. B. MacQuarrie[1], and Clifford I. Voss[2]

[1]Department of Civil Engineering and Canadian Rivers Institute, University of New Brunswick, Fredericton, New Brunswick, Canada, [2]U.S. Geological Survey, Menlo Park, California, USA

Abstract Cold groundwater discharge to streams and rivers can provide critical thermal refuge for threatened salmonids and other aquatic species during warm summer periods. Climate change may influence groundwater temperature and flow rates, which may in turn impact riverine ecosystems. This study evaluates the potential impact of climate change on the timing, magnitude, and temperature of groundwater discharge from small, unconfined aquifers that undergo seasonal freezing and thawing. Seven downscaled climate scenarios for 2046–2065 were utilized to drive surficial water and energy balance models (HELP3 and ForHyM2) to obtain future projections for daily ground surface temperature and groundwater recharge. These future surface conditions were then applied as boundary conditions to drive subsurface simulations of variably saturated groundwater flow and energy transport. The subsurface simulations were performed with the U.S. Geological Survey finite element model SUTRA that was recently modified to include the dynamic freeze-thaw process. The SUTRA simulations indicate a potential rise in the magnitude (up to 34%) and temperature (up to 3.6°C) of groundwater discharge to the adjacent river during the summer months due to projected increases in air temperature and precipitation. The thermal response of groundwater to climate change is shown to be strongly dependent on the aquifer dimensions. Thus, the simulations demonstrate that the thermal sensitivity of aquifers and baseflow-dominated streams to decadal climate change may be more complex than previously thought. Furthermore, the results indicate that the probability of exceeding critical temperature thresholds within groundwater-sourced thermal refugia may significantly increase under the most extreme climate scenarios.

1. Introduction

Spatially discrete groundwater discharge can induce riverine thermal heterogeneity and thereby create microhabitats for cold water fishes during high-temperature events [e.g., *Ebersole et al*., 2003; *Torgersen et al*., 1999; *Goniea et al*., 2006; *Torgersen et al*., 2012]. These cold water plumes, known as thermal refugia, enable fish to survive in river reaches that would otherwise be thermally uninhabitable [*Sutton et al*., 2007]. Thermal refugia generated by groundwater discharge from adjacent/underlying aquifers have been observed at geographically diverse locations and for various aquatic species [e.g., *Bilby*, 1984; *Nielsen et al*., 1994; *Biro*, 1998; *Olsen and Young*, 2009; *Befus et al*., 2013; *Briggs et al*., 2013; *Bunt et al*., 2013; *Dugdale et al*., 2013]. Furthermore, the thermal regimes of shallow, unconfined aquifers are of ecological importance because diffuse groundwater discharge can buffer seasonal or diel variability in ambient river water temperatures [*Hayashi and Rosenberry*, 2002; *Story et al*., 2003; *Caissie*, 2006]. Buffering occurs because groundwater temperature exhibits less seasonal variability than surface water temperature due to the heat capacity of the overlying soil and the insulation from solar radiation [*Bonan*, 2008].

Global climate models (GCMs) project significant shifts in global and regional air temperature (AT) and precipitation regimes [*Meehl et al*., 2007a, 2007b]. These changing meteorological conditions will likely result in rising surface water temperatures and a corresponding loss of habitat for cold water fish species [*Chu et al*., 2005; *Webb et al*., 2008; *Jonsson and Jonsson*, 2009; *van Vliet et al*., 2011, 2013; *Wu et al*., 2012; *Moore et al*., 2013; *Jones et al*., 2013]. The increased thermal stress on lotic ecosystems is expected to magnify salmonid reliance on groundwater-sourced thermal refugia [*Brewer*, 2013], particularly at the lower elevational or latitudinal limits of their distributions. Several researchers have acknowledged the need for further studies investigating the influence of climate change on groundwater temperature and/or groundwater discharge rates [e.g., *Mohseni et al*., 2003; *Chu et al*., 2008; *Mayer*, 2012]. *Kanno et al*. [2013] noted that the "spatial

variability in resiliency of groundwater temperature in response to air temperature is the critical missing piece to assess climate change impacts on headwater stream fish accurately."

Research examining relationships between climate change and groundwater temperature and flow rates is limited, and knowledge gaps remain. First, previous studies investigating the effects of climate change on groundwater were primarily focused on groundwater resources, largely ignoring subsurface thermal response to climate change [see reviews by *Green et al*., 2011; *Taylor et al*., 2013; *Kurylyk and MacQuarrie*, 2013]. Second, most studies that have considered the thermal evolution of aquifers due to future climate change employed simplified one-dimensional analytical solutions to conduction-advection heat transport equations [e.g., *Gunawardhana et al*., 2011; *Kurylyk and MacQuarrie*, 2014]. One-dimensional solutions have limited ability to simulate groundwater flow and heat transport in shallow aquifers, because both thermal and hydraulic processes are typically multidimensional. Also, existing analytical solutions to the conduction-advection equation that consider climate change influence on groundwater temperature ignore seasonal changes in surface and subsurface temperature. Other analytical solution studies have assumed that conduction is the only significant heat transport process controlling the thermal response of groundwater to climate change [e.g., *Taylor and Stefan*, 2009]; however, heat advection due to groundwater flow can significantly perturb the conductive thermal regime in some subsurface environments [*Woodbury and Smith*, 1985]. Third, the few climate change-groundwater temperature studies that have utilized multidimensional models were focused on relationships between permafrost degradation and aquifer reactivation [e.g., *Bense et al*., 2009; *Painter*, 2011; *Frampton et al*., 2013; *McKenzie and Voss*, 2013]. These were conducted for high latitude/altitude climates and did not detail effects of aquifer warming on riverine ecosystems. Finally, previous studies typically employed simplified climate change scenarios (e.g., a linear increase in surface temperature) rather than downscaled GCM output. Simplified scenarios may overlook complex relationships between atmospheric climate change and groundwater temperature, such as the subsurface thermal influence of changing groundwater recharge patterns and snowpack evolution.

The objective of this paper is to investigate the influence of climate change on the characteristics of groundwater discharge from shallow, unconfined aquifers to streams or rivers. In particular, we consider changes to the timing, magnitude, and temperature of groundwater discharge.

The investigations are conducted in the context of the climate, hydrology, and hydrogeology of central New Brunswick, Canada. The hydraulic and thermal sensitivities of unconfined aquifers to climate change are simulated by driving surface energy and water balance models with downscaled climate model output and then applying the output from these surface models as boundary conditions for a groundwater flow and heat transport model. Unlike most previous studies, the groundwater discharge and temperature projections are investigated on both a mean annual and seasonal basis. The ecological implications are evaluated by considering simulated changes to the timing, magnitude, and temperature of groundwater discharge in the context of existing thermal refugia conditions and previously established salmonid thermal tolerances. Particular emphasis is placed on the summer period when the existence of thermal refugia can be critical for riverine ecosystem complexity.

To our knowledge, this is the first study to utilize daily downscaled climate projections to investigate climate change impacts to aquifer thermal and hydraulic regimes. The study of future climate change impacts is becoming increasingly multidisciplinary [*Meehl et al*., 2007a], and it is important that groundwater hydrologists also progress toward the integration of GCM simulations with groundwater flow and energy transport modeling. Thus, we improve on the conventional practice of driving subsurface energy transport models with climate trends that are only loosely derived from GCM output and align our methodology with river temperature analysts who utilize actual downscaled GCM output. This contribution, which employs a process-oriented groundwater flow and energy transport model, expands on a recent study that utilized an empirical groundwater temperature model to investigate shallow groundwater temperature response to climate change [*Kurylyk et al*., 2013].

2. Site Description and Conceptual Model

The present study is focused on groundwater-sourced thermal refugia within the Miramichi River system in New Brunswick, Canada, which is the largest producer of wild Atlantic salmon (*Salmo salar*) in North America [*Caissie et al*., 2007]. In New Brunswick, summer river temperatures are currently approaching the

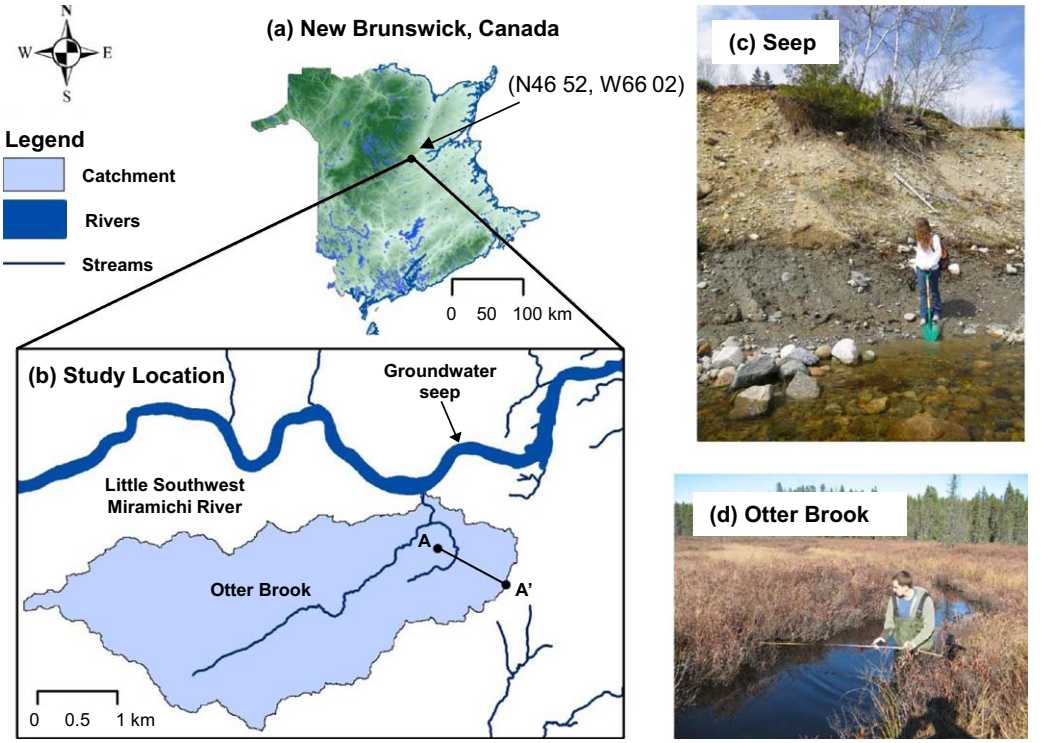

Figure 1. Study site. (b–d) The locations of the Little Southwest Miramichi River, Otter Brook, and the groundwater seep are shown with respect to their location in (a) New Brunswick, Canada (map data from *NBADW* [2011]). The coordinates for Otter Brook are N46 52 W66 02.

critical threshold for salmonids [*Breau et al*., 2007; *Cunjak et al*., 2013], and discrete cold water plumes formed by groundwater-surface water interactions have been shown to provide critical thermal refuge for salmonids in the Miramichi River system [*Cunjak et al*., 2005; *Breau et al*., 2007, 2011; *Monk et al*., 2013]. The Little Southwest Miramichi River (LSW) is a fifth-order branch of the Miramichi River located in central New Brunswick, Canada (Figure 1) that experiences a humid-continental climate characterized by arid, cold winters [*Cunjak et al*., 1993]. Annual precipitation is 1230 mm, with ~33% falling as snow [*Environment Canada* (*EC*), 2013]. The LSW is a relatively wide, shallow river with a width to depth ratio of ~150. Thus, it responds rapidly to summer radiation, with water temperatures occasionally exceeding 30°C.

An airborne infrared thermal survey of the LSW [*Wilbur and Curry*, 2011] identified numerous thermal anomalies, including one on the south side of the LSW at the mouth of a cold, baseflow-dominated tributary (Otter Brook, N46 52 W66 02) and one on the north side of the LSW at a lateral groundwater seep (Figure 1). A thermal infrared image of the LSW and the thermal refugia at the groundwater seep and the mouth of Otter Brook is included in supporting information (Figure fs01). These identified refugia are biologically important. For example, the refuge at the mouth of Otter Brook (Figure 1) accommodated ~6000 to10,000 juvenile Atlantic salmon simultaneously in July 2010 when LSW temperatures exceeded 30°C (*Linnansaari*, UNB, personal communication, 2013). These field observations of unconfined, alluvial aquifers generating thermal refugia form the motivation and conceptual models for the present study.

The unconfined aquifers that provide groundwater discharge to Otter Brook and the lateral groundwater seep were conceptualized as being two-dimensional (cross sections) and homogeneous. The thermal and hydraulic properties of the aquifers were derived from field observations of surface and subsurface conditions in these catchments. The Otter Brook and groundwater seep deposits are primarily composed of highly permeable glaciofluvial outwash sediments, varying from cross-bedded sand to thick-bedded coarse gravel [*Allard*, 2008]. Aquifer hydraulic properties were established from grain size analyses conducted by *Allard* [2008] in conjunction with the methodology proposed by *Hazen* [1911]. More details are provided in the supporting information (text01).

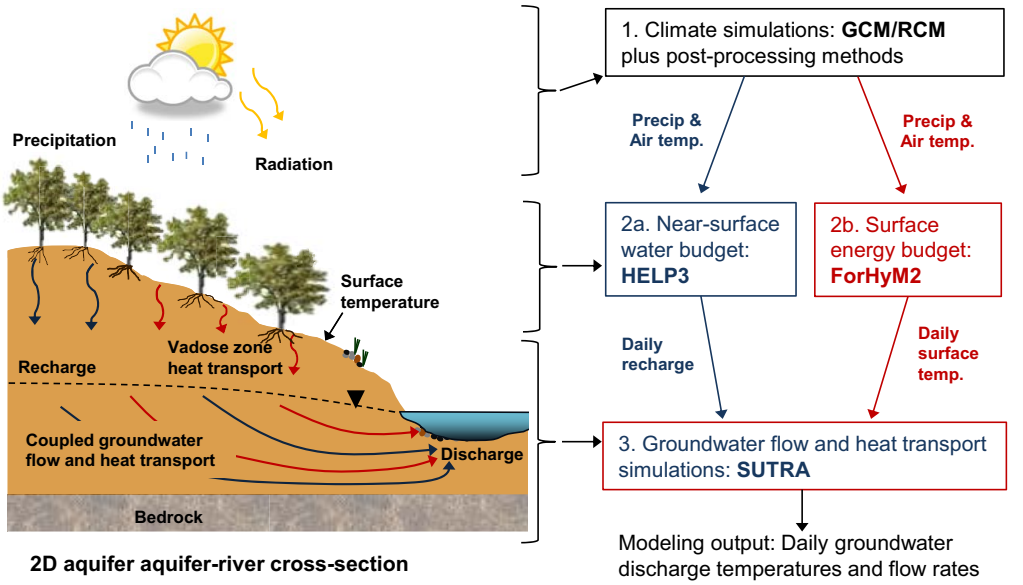

Figure 2. (left) The physical processes generating groundwater-sourced thermal refugia and (right) the associated modeling sequence. Climate data are utilized to drive surface simulations of the energy and water budget, and the results from the surface simulations form the boundary conditions for the variably saturated groundwater flow and heat transport model.

Dimensions of the aquifers contributing to the groundwater seep and Otter Brook were estimated from a digital elevation model [*New Brunswick Aquatic Data Warehouse* (*NBADW*), 2011] and/or GPR surveys [*Allard*, 2008]. Although Otter Brook diverges into two branches ~650 m upstream of its mouth (Figure 1b), the brook was conceptualized as a single symmetrical branch with an outwash deposit on either side. Section A-A′ (Figure 1b) was chosen as the simulation cross section for the Otter Brook deposit because surface water thermal surveys indicated significant groundwater discharge in this region. Because the Otter Brook catchment is a marshy environment (Figure 1d), the depth of groundwater discharge to Otter Brook is near the ground surface. The aquifer discharging to the groundwater seep is underlain by a gray clay aquitard (Figure 1c) that forces the groundwater seep to discharge at an elevation above the LSW water surface. Due to the steep vertical bank on the north side of the LSW, the depth of the seep discharge is on average 7 m below the ground surface. These two distinct aquifer configurations were selected to investigate the influence of an aquifer's dimensions on its hydraulic and thermal response to atmospheric climate change. The idealized aquifers representing the hydrogeological units discharging to Otter Brook and the groundwater seep are hereafter referred to as "Configuration 1" and "Configuration 2," respectively. Our intent is not to make definitive predictions regarding the future states of these two particular aquifers, but rather to assess the sensitivity of representative, thermal refugia-generating aquifers to external climatic forcing.

3. Numerical Simulation Approach

The physical processes that generate groundwater-sourced thermal refugia and the associated overall modeling sequence employed in the present study are depicted in Figure 2. Atmospheric processes drive hydraulic and thermal exchanges across the ground surface, and these surface processes in turn control subsurface conditions. The combined effects of these physical processes can be simulated in a sequential manner by linking physically based models for the lower atmosphere, ground surface, and shallow subsurface (Figure 2). In the present study, surface simulations were performed independently of subsurface simulations. The modeling processes shown in steps 2a, 2b, and 2c of Figure 2 are described in subsequent sections.

3.1. Climate Data

Daily observed climate data (AT and precipitation) for 1961–2000 were obtained for the LSW region from the EC adjusted and homogenized daily climate database [*Environment Canada* (*EC*), 2011]. These observed

Table 1. Details for the Climate Scenarios Utilized in This Study

Emission Scenario	Model Type	Model Name	GCM Driver	ID	Postprocessing Method	Contributor Organization
A2	GCM	CGCM3			Statistical-HMR	INRS [*Jeong et al*., 2012a]
A2	RCM	CRCM 4.2.3	CGCM3	Aev	Dynamical	Ouranos [*Huard*, 2011]
A2	RCM	CRCM 4.2.3	Echam5	Agx	Dynamical	Ouranos [*Huard*, 2011]
B1	GCM	CSIRO Mk3.0			Statistical-DT	Ouranos [*Huard*, 2011]
B1	GCM	CSIRO Mk3.5			Statistical-DT	Ouranos [*Huard*, 2011]
A1B	GCM	Miroc3.2Hires			Statistical-DT	Ouranos [*Huard*, 2011]
A1B	GCM	CGCM3			Statistical-HMR	INRS [*Jeong et al*., 2012a]

climate data were utilized to drive reference period simulations of surface processes to form a datum from which to evaluate the sensitivity to future climate change (Figures 2a and 2b).

Coarse-resolution GCM projections are often statistically downscaled [*Chen et al*., 2012; *Jeong et al*., 2012b] or dynamically downscaled with regional climate models (RCMs) [*Boe et al*., 2007; *de Elia et al*., 2008] and further debiased [*Teutschbein and Seibert*, 2012] to produce projections of local climate data and hydrology. For the present study, seven projected climate scenarios (Table 1) were produced for the period of 2046–2065 using six GCMs, two downscaling methods, and three emission scenarios. Two downscaled climate scenarios were obtained via hybrid multiple regression statistical downscaling approaches (HMR) [*Jeong et al*., 2012a, 2012b]. These climate series were contributed by the Université du Québec Institut National de la Recherche Scientifique (INRS) (D. Jeong, personal communication, 2011). The other climate data series were produced from the third Coupled Model Intercomparison Project database of GCM output (CMIP3) [*Meehl et al*., 2007b] and statistically downscaled with the daily translation (DT) method or dynamically downscaled using the Canadian Regional Climate Model (CRCM4.2.3) [*de Elia et al*., 2008] and further processed [*Huard*, 2011]. The "ID" in Table 1 refers to a particular RCM simulation and GCM driver. These climate series are further described in *Kurylyk and MacQuarrie* [2013].

The climate series span the range of plausible projected changes in local mean annual AT (range among climate scenarios of $+0.4$ to $+3.9$°C, mean $+2.1$°C) and precipitation (range of -12% to $+49$%, mean $+8$%) for 2046-2065 compared to the 1961–2000 observed climate data (Figure 3a).

3.2. Surface and Near-Surface Modeling of Recharge and Ground Surface Temperature

The observed climate data from 1961 to 2000 [*EC*, 2011] and the climate scenarios given in Table 1 were utilized to drive simulations within the hydrological model HELP3 (Hydrologic Evaluation of Landfill Performance) [*Schroeder et al*., 1994] to obtain future projections of daily groundwater recharge (Step 2a, Figure 2). HELP3 is a quasi-two-dimensional daily soil water balance model capable of simulating the influence of changing climatic conditions on surface and shallow subsurface hydrological processes, including snowpack accumulation and melt [e.g., *Allen et al*., 2010; *Crosbie et al*., 2011]. In HELP3, precipitation accumulates as snowpack during the winter months when AT is low causing a seasonal cessation of recharge. HELP3 also simulates a decrease in late fall and early spring recharge by increasing the runoff curve number during periods when air temperatures are low and soil is presumed to be frozen. Additional information describing the HELP3 modeling process can be found in *Kurylyk and MacQuarrie* [2013]. The HELP3 simulations indicate that projected changes to future mean annual groundwater recharge for each climate series vary significantly (range of -6% to $+58$%, mean $+18$% for 2046–2065 compared to the recharge simulation using observed climate data, Figure 3b). These simulations also indicate that spring snowmelt and the consequent major recharge event will likely occur earlier in the year due to increases in winter and early spring AT [*Kurylyk and MacQuarrie*, 2013].

The observed and projected climate series (Table 1) were also utilized to drive simulations within the surface energy flux balance model ForHyM2 (Forest Hydrology Model) [*Yin and Arp*, 1993] to obtain future projections of daily ground surface temperature (GST, Step 2b, Figure 2). ForHyM2 is a water and energy transport model that simulates surficial energy fluxes (e.g., shortwave and longwave radiation and convective exchanges) and near-surface heat transport via conduction through multiple layers (forest canopy, snowpack, forest floor, soil, and subsoil) [*Yin and Arp*, 1993; *Balland et al*., 2006]. ForHyM2 was only applied to obtain GST for the present study, as the model is one-dimensional and does not accommodate subsurface advective heat transport. ForHyM2-simulated daily GST agree closely (mean error = 0.02°C) with field

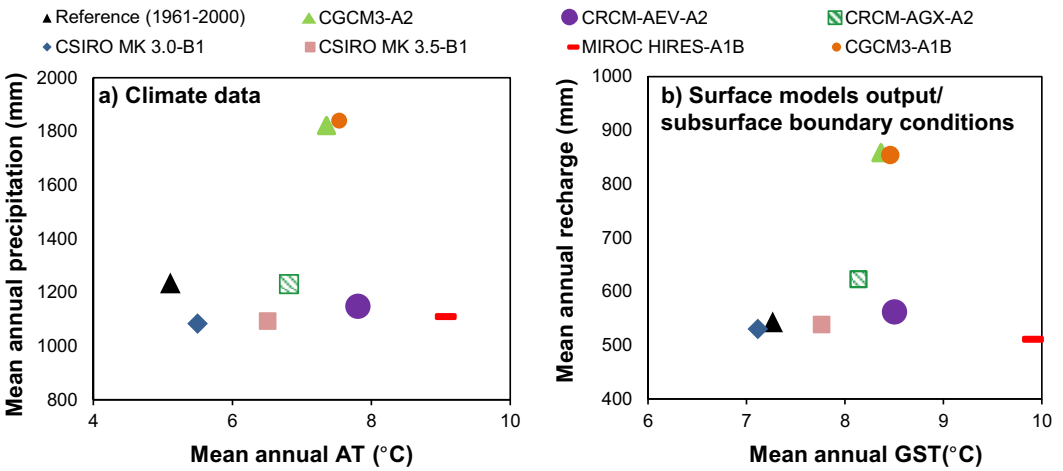

Figure 3. (a) The observed/reference (1961–2000) and projected (2046–2065) mean annual AT and precipitation (see Table 1) and (b) the mean annual groundwater recharge and GST simulated by driving surface models HELP3 and ForhyM2 with the climate data shown in Figure 3a.

observations of GST during both snow-covered and snow-free periods [*Kurylyk et al*., 2013, Figure 4]. ForHyM2 simulations for the projected climate scenarios suggest that changes to average summer GST (mean among climate scenarios of +1.49°C compared to the 1961–2000 simulation) will generally follow average summer AT changes. However, projected increases in winter AT (mean +3.04°C) will result in decreased winter GST (mean −0.53°C) due to a reduction in the winter snowpack and its insulating capabilities. As Figure 3b illustrates, the decrease in simulated winter GST results in simulated average annual GST changes (mean +1.06°C) that are damped compared to the projected increases in average annual AT (mean +2.1°C). Further details related to the ForHyM2 modeling process and results can be found in *Kurylyk et al*. [2013].

Note that the details given by *Kurylyk et al*. [2013] relate to simulations performed for the Catamaran Brook catchment, which is a small catchment adjacent to Otter Brook. Because of the geographical proximity and similar surface and shallow subsurface conditions, the GST simulations performed for the Catamaran Brook

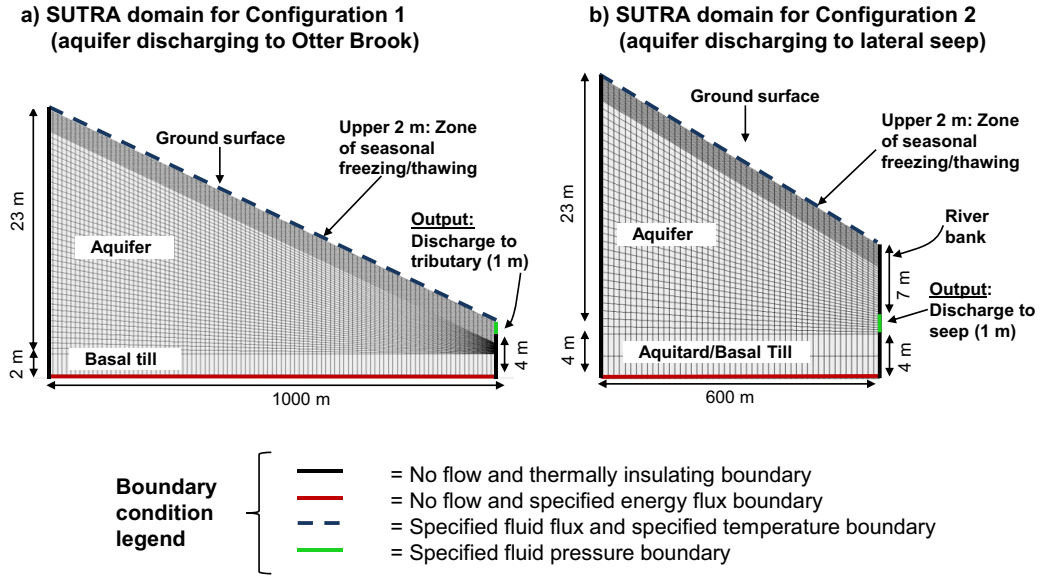

Figure 4. SUTRA aquifer configurations and boundary conditions for (a) Configuration 1 and (b) Configuration 2. Vertical exaggeration is ~25:1. The finite element meshes employed in SUTRA were much denser than those shown above (see supporting information, text01).

catchment were assumed to also represent current and projected GST trends in the Otter Brook catchment and the lateral groundwater seep catchment (Figure 1). Similarly, the current and projected recharge simulated for the Otter Brook catchment [*Kurylyk and MacQuarrie*, 2013] are also assumed to be representative of the current and future recharge regimes in the groundwater seep catchment due to the similar surface and shallow subsurface conditions [*Allard*, 2008].

3.3. Groundwater Flow and Heat Transport Model

3.3.1. Model Selection

Due to the noted limitations inherent in analytical solutions, a numerical model was employed to simulate the impacts of atmospheric and surficial climate change on the timing, magnitude, and temperature of groundwater discharge from shallow, unconfined aquifers. Pore ice formation can impact groundwater discharge conditions where significant seasonal freezing occurs. For example, the latent heat released or absorbed during pore water freeze-thaw usually dominates conductive and advective heat transport in the zone of freezing and significantly retards the propagation of surface temperature signals during the early winter freeze and spring thaw [*Woo*, 2012]. Furthermore, pore ice formation reduces hydraulic conductivity and impedes groundwater flow [*Watanabe and Wake*, 2008; *Kurylyk and Watanabe*, 2013]. The model selected for the present study, SUTRA, is a multidimensional finite element model of coupled groundwater flow and heat transport [*Voss and Provost*, 2002] that has been modified by *McKenzie et al*. [2007] to accommodate freezing and thawing processes for saturated conditions, and then recently enhanced to allow for variably saturated conditions during freezing and thawing. In addition to accommodating the dynamic freeze-thaw process, SUTRA simulates subsurface heat transport via conduction, advection, and thermal dispersion, allowing pore water flow due to gradients in pressure, elevation, and water density [*Voss and Provost*, 2002]. The governing water flow and heat transport equations, model parameterization (thermal and hydraulic properties, relative permeability function, soil drying curve, and soil freezing curve) and model controls (mesh density, time step size, and solver settings) are given in supporting information (text01).

3.3.2. SUTRA Boundary Conditions and Run Information

Figure 4 depicts the boundary conditions and domains for the SUTRA simulations. Both aquifers were assigned no-flow hydraulic boundaries and perfectly insulating thermal boundaries at the groundwater divide (left vertical boundaries, Figure 4). The bottom boundary was specified as a no-flow boundary condition for both configurations. A specified heat flux (0.060 $W \cdot m^{-2}$) was also assigned to this boundary to represent the geothermal heat flux from greater depths [e.g., *Bense et al*., 2009]. The discharge location for both configurations was represented as a specified pressure boundary condition. For Configuration 1, this pressure increased linearly with depth (1 m) to represent hydrostatic pressure within Otter Brook.

The surface boundaries for both aquifers were assigned specified temperature (GST) and specified fluid flux (groundwater recharge) boundary conditions, with recharging water having the same temperature as the ground surface. By directly specifying the GST output from ForHyM2, it was possible to simulate subsurface responses to complex atmosphere-surface interactions (e.g., snowpack accumulation, insulation, and ablation). A specified groundwater recharge boundary condition is preferred to a specified-pressure boundary condition if, as in this case, the recharge is climate-controlled [*Sanford*, 2002]. This approach allows for a natural groundwater table and unsaturated zone to develop. Recharge, rather than infiltration, was specified along the ground surface boundary because this version of SUTRA does not include evapotranspiration.

SUTRA simulations were performed with fine temporal and spatial scales (constant time step = 4.8 h (0.2 days), minimum element height = 0.03 m). The model predicts the volumetric liquid and ice saturations, temperature, and pore water pressure at every time step for each node in the model domain (85,170 and 62,300 nodes for Configurations 1 and 2, respectively) and groundwater velocity for every element. Table 2 lists the details of each simulation performed. Reference period simulations (runs R.1 and R.2) were performed to establish a baseline from which to measure projected future changes in the timing, magnitude, and temperature of groundwater discharge (runs 1.1–7.2). Runs 8.1–9.2 were performed to investigate the thermal influence of advection and pore water phase change and thereby determine the suitability of

Table 2. Details for Each Simulation Performed in SUTRA

Run ID[a]	Climate Scenario	Advection On?	Freezing On?[b]
Init. Cond.[c]	Ref. (1961–1981)	Yes	Yes
R.1 and R.2	Ref. (1981–2000)	Yes	Yes
1.1 and 1.2	CGCM3-A2[d]	Yes	Yes
2.1 and 2.2	CRCM4.2.3-aev	Yes	Yes
3.1 and 3.2	CRCM4.2.3-agx	Yes	Yes
4.1 and 4.2	CSIRO Mk3.0	Yes	Yes
5.1 and 5.2	CSIRO Mk3.5	Yes	Yes
6.1 and 6.2	Miroc3.2Hires	Yes	Yes
7.1 and 7.2	CGCM3-A1B	Yes	Yes
8.1 and 8.2	Ref. (1981–2000)	No	Yes
9.1 and 9.2	Ref. (1981–2000)	Yes	No

[a]The number following the decimal point in the Run ID refers to the aquifer configuration. For example, Run 1.1 is Run 1 (i.e., the CGCM3-A2 climate scenario with advection and freezing on) for Configuration 1.

[b]"Freezing" refers to the subroutine in SUTRA to accommodate pore water freezing.

[c]"Init. Cond." refers to initial conditions, which were generated by first running simulations for 40 years with observed climate data (1961–2000) and then using those conditions to start a subsequent run driven by 1961–1980 climate data. The 1961–1980 simulation results formed the initial conditions for each of the other runs indicated in Table 2.

[d]The period for each of the future climate scenarios was 2046–2065 (see Table 1).

employing simplified models (i.e., conduction-only) to predict the response of shallow groundwater to climate change.

4. Results

4.1. Seasonal and Long-Term Changes to Groundwater Discharge Temperature

Figure 5 shows measured AT and simulated GST and groundwater discharge temperature for both aquifer configurations averaged for each calendar day over the 20 year reference period (1981–2000, SUTRA runs R.1 and R.2 in Table 2). The presence of the insulating snowpack clearly decouples winter AT and GST trends. The groundwater discharge temperatures presented in Figure 5 and subsequent figures were obtained from the bottom node of the discharge boundary (specified pressure boundary, Figure 4). Temperatures at the discharge boundary were shown to be relatively uniform due to high groundwater flows (advection) and concomitant high dispersion.

The groundwater discharge temperatures for Configuration 2 are characterized by more damping and lagging than the groundwater discharge temperatures for Configuration 1 due to the increased depth of the discharge point in Configuration 2 (Figure 4). A groundwater discharge thermal damping factor can be defined as the ratio of the amplitude of the annual groundwater discharge temperature cycle to the amplitude of the annual GST cycle. For the reference period simulation, the average amplitudes of the annual groundwater discharge temperature cycles are 8.3°C and 2.1°C for Configurations 1 and 2, respectively, whereas the amplitude of the annual GST cycle is 11.6°C (Figure 5). Thus, the attenuation of the seasonal GST cycle for the discharge point of Configuration 2 (damping factor = 0.18) is approximately four times that of Configuration 1 (damping factor = 0.72). Figures 5 and 6 also indicate that the maximum groundwater discharge temperature for the reference period simulations occurs on days of the year (DOY) 223 and 303 for Configurations 1 and 2, respectively. This indicates that the groundwater discharge temperature signal is lagged an additional 80 days for Configuration 2.

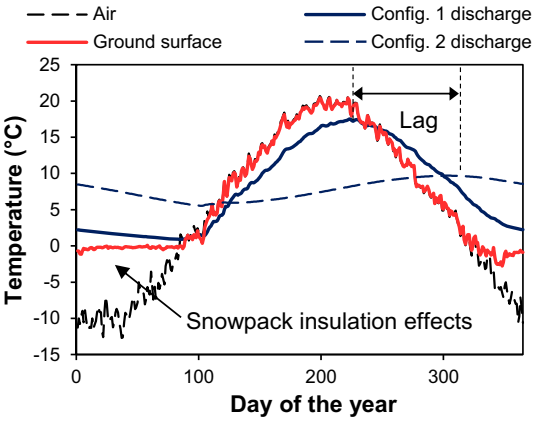

Figure 5. Measured AT, ForHyM2-simulated GST, and SUTRA-simulated groundwater discharge temperature for both aquifer configurations averaged for each day of the year during the reference period (1981–2000, Runs R.1 and R.2, Table 2). Although not depicted in these results, the AT and GST exhibit considerable diel variability, whereas the groundwater discharge temperature, even for Configuration 1, is constant throughout the day.

Figure 6 depicts the simulated groundwater discharge temperatures for the reference period (SUTRA runs R.1 and R.2, Table 2) and the future period (SUTRA runs 1.1–7.2). The future period simulations shown in Figure 6 are generally characterized by higher groundwater discharge temperatures that are shifted slightly earlier in the year. For example, the warmest climate scenario (MIROC-HIRES-A1B) results in a

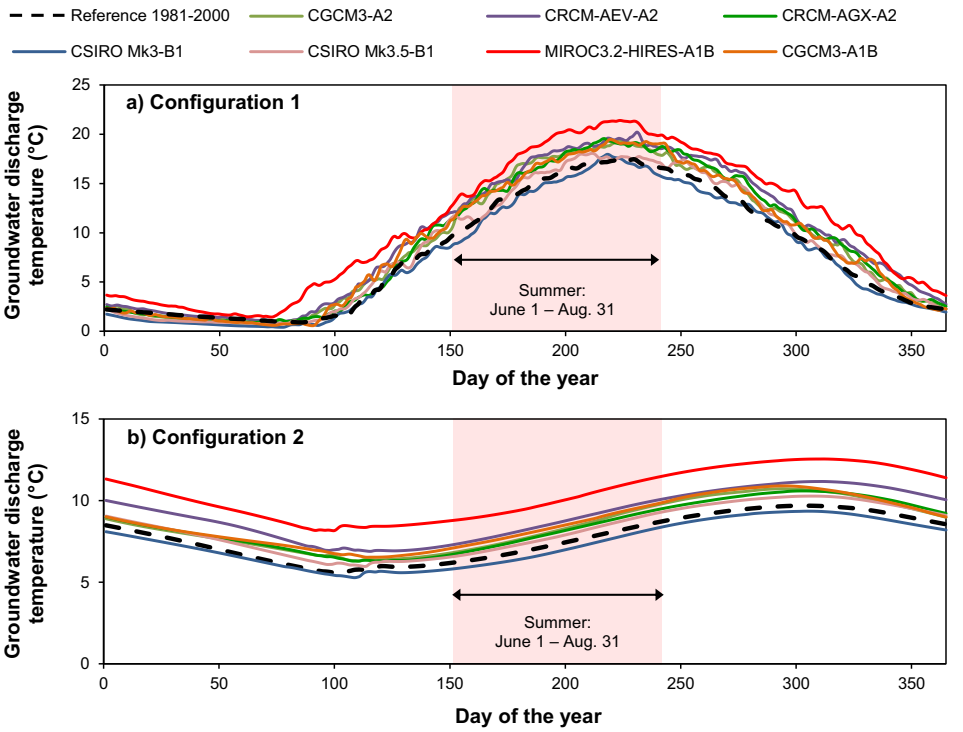

Figure 6. Simulated groundwater discharge temperature for (a) Configuration 1 and (b) Configuration 2. Results are shown for the reference period (runs R.1 and R.2, Table 2) and for the last 10 years (2056–2065) of data for each of the climate scenarios given in Table 1 (runs 1.1–7.2, Table 2). The results are averaged over the simulation period for each day of the year. The two plots are drawn to different scales.

maximum groundwater discharge temperature for Configuration 1 that is 3.3°C higher than that simulated for the reference period simulation.

The climate change-induced increases in groundwater discharge temperature simulated for each calendar day for Configuration 2 are relatively constant and approximate the increase in mean annual GST for each climate scenario (see supporting information Figure fs02). However, the simulated changes in daily groundwater discharge temperatures for Configuration 1 are characterized by considerable daily variability.

4.2. Influence of Advection and Pore Water Phase Change

Heat advection via groundwater flow can significantly perturb subsurface thermal environments [*McKenzie and Voss*, 2013; *Kurylyk and MacQuarrie*, 2014]. Also the latent heat released or absorbed during freezing or thawing greatly increases the subsurface effective heat capacity and thereby attenuates high-frequency GST signals. In addition to releasing/absorbing latent heat and impeding heat advection, the dynamic freeze-thaw process can also influence subsurface thermal regimes by altering the bulk thermal diffusivity (thermal conductivity/heat capacity) of the porous medium, as the thermal diffusivity of ice is ~8 times that of water [*Bonan*, 2008]. To test the subsurface thermal influence of groundwater flow and pore water phase change, separate reference period simulations were performed for both aquifer configurations without considering the effects of advection (SUTRA runs 8.1 and 8.2, Table 2) or the dynamic freeze-thaw process (SUTRA runs 9.1 and 9.2).

Figure 7 demonstrates the thermal influence of groundwater flow in Configuration 1 for the reference period. The temperatures at the specified pressure boundary condition (i.e., the location of groundwater discharge when flow is activated) were compared for the simulations including (run R.1) and neglecting (run 8.1) the thermal influence of advection. Because groundwater flow primarily occurs during the warmer months and abates during the winter months, the outlet temperatures for the simulation neglecting advection are generally colder (maximum difference = 3.1°C) than the groundwater discharge temperatures for the simulation with advection considered.

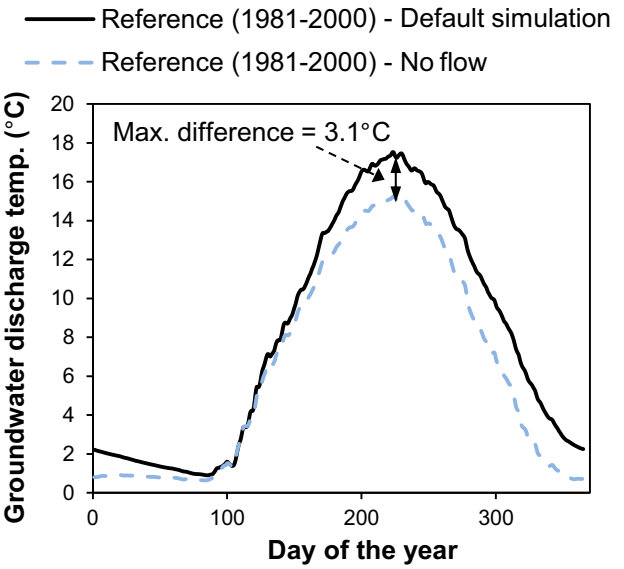

Figure 7. Simulated groundwater discharge temperature versus the day of the year for Configuration 1. Results are presented for the default simulation for the reference period (run R.1, Table 2) and a simulation with no recharge applied (run 8.1). Results are averaged for each day of the year over the reference period.

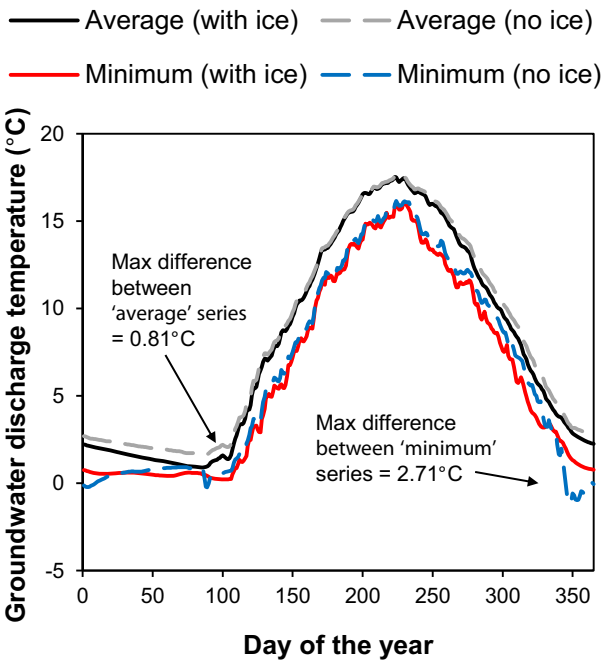

Figure 8. Configuration 1 groundwater discharge temperature versus the day of the year for the reference period simulation (1981–2000). Solid lines indicate the results for when the effects of ice were considered (run R.1, Table 2), and the dashed lines indicate the simulation results when the effects of ice were not included (run 9.1). Results are presented for the discharge temperature averaged for each day of the year over the 20 year simulation and for the minimum discharge temperature simulated for each day of the year.

Figure 8 shows the results for the reference period Configuration 1 simulations performed with (run R.1) and without (run 9.1) the influence of pore water phase change considered. The results demonstrate that the inclusion of the freeze-thaw process can significantly impact the groundwater discharge temperature in a given year, but that its influence is reduced in this aquifer when the results are averaged over the 20 year simulation. For example, the maximum difference between the two series representing the minimum groundwater discharge temperature for each calendar day is 2.71°C, but this difference decreases to 0.81°C when the results are averaged for each calendar day of the simulation.

Temperature profiles were also analyzed halfway up the hillslope in Configuration 1 (i.e., 500 m from the outlet, Figure 4a) to investigate the impact of the dynamic freeze-thaw process at locations other than the discharge location. The results, which are shown in Figure fs03 of the supporting information, indicate that the maximum difference between the simulated groundwater temperatures at 1 m depth with and without the effects of freeze-thaw considered (i.e., runs R.1 and 9.1) was 4.03°C. This difference is significant, given that this value is ~50% of the amplitude of the annual groundwater temperature cycle at this depth. However, the thermal influence of freeze-thaw is quickly attenuated with depth and is barely discernible at depths greater than 4 m in this aquifer. In general, the results presented in Figures 7 and 8 and the supporting information indicate that properly accounting for the thermal influence of advection and pore water phase change is most important in the shallow subsurface of the LSW catchment.

4.3. Simulated Groundwater Discharge Magnitude and Timing

Figure 9 presents simulated reference period daily groundwater recharge and discharge for both aquifer

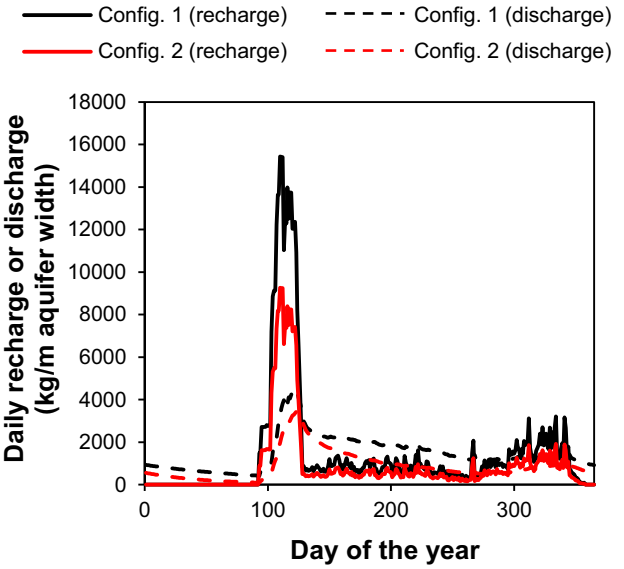

Figure 9. Simulated groundwater recharge and discharge per meter aquifer width for Configuration 1 (SUTRA run R.1, Table 2) and Configuration 2 (run R.2) averaged for each day of the year for the reference period.

configurations. In general, the groundwater discharge per unit width from Configuration 1 exceeds the groundwater discharge per unit width from Configuration 2 due to their differing aquifer lengths (1000 and 600 m, Figure 4). Figure 9 indicates that the magnitude and timing of groundwater discharge from these highly permeable aquifers is strongly controlled by intra-annual groundwater recharge. For example, the timing of the maximum groundwater discharge rate for the reference period simulation lags the timing of the maximum recharge rate by only 13 and 14 days for Configurations 1 and 2, respectively. The average annual total recharge masses (534,000 kg and 320,000 kg for Configurations 1 and 2 per meter aquifer width) are approximately equal to the average annual total discharge masses (538,000 kg and 322,000 kg for Configurations 1 and 2 per meter aquifer width). There are, however, discernible differences between the seasonal recharge and discharge rates shown in Figure 9. Due to subsurface hydraulic storage properties, the temporal variability of groundwater discharge is damped in comparison to the temporal variability of groundwater recharge. For example, groundwater recharge exceeds discharge during the spring months. This accumulated water is slowly released from the aquifers during the summer months when discharge typically exceeds recharge (Figure 9). Similarly, late fall recharge exceeds discharge, and this water is released during the winter when recharge ceases during snowpack accumulation [*Kurylyk and MacQuarrie*, 2013].

Figure 10 shows the simulated groundwater discharge rates for both aquifer configurations for the reference period and future climate series. In general, the future period simulations exhibit increases or decreases in average groundwater discharge rates that correspond to the simulated increases or decreases in average annual recharge (Figure 3b). Some similarities exist between reference period and future period simulations. For example, Figure 10 shows that a major discharge event occurs in the spring as a result of snowmelt. These peak daily discharges range from 3855 kg (MIROC-HIRES-A1B) to 6846 kg (CGCM3-A1B) per meter width for Configuration 1, and 2843 kg (CRCM-AEV-A2) to 4668 kg (CGCM3-A1B) for Configuration 2. Each series in Figure 10 exhibits a distinct decreasing trend in discharge during the summer months (June–August) arising from the abatement of summer recharge due to reduced precipitation and increased evapotranspiration [*Kurylyk and MacQuarrie*, 2013]. Each simulation also includes a smaller groundwater discharge event corresponding to the late-fall rainy season and a reduction in groundwater discharge during the winter months due to recharge cessation.

5. Discussion

5.1. Changes to the Mean and Amplitude of the Groundwater Discharge Temperature Cycle

The simulated mean annual groundwater discharge temperature trends for each climate scenario generally follow the trends in projected mean annual GST (Figures 3 and 6). For example, the MIROC3.2-HIRES-A1B climate series simulations (run 6.1) are characterized by the largest increases in mean annual AT (+3.96°C, Figure 3a) and mean annual GST (+2.65°C, Figure 3b) compared to the reference period, and this climate scenario is also characterized by the most pronounced increases in mean annual groundwater discharge temperature (+2.85°C and +2.70°C for Configurations 1 and 2, respectively). The SUTRA simulation results for the CSIRO Mk3-B1 scenario exhibit slight decreases in both the mean annual groundwater discharge temperature (−0.45°C and −0.33°C for Configurations 1 and 2, respectively) and summer groundwater

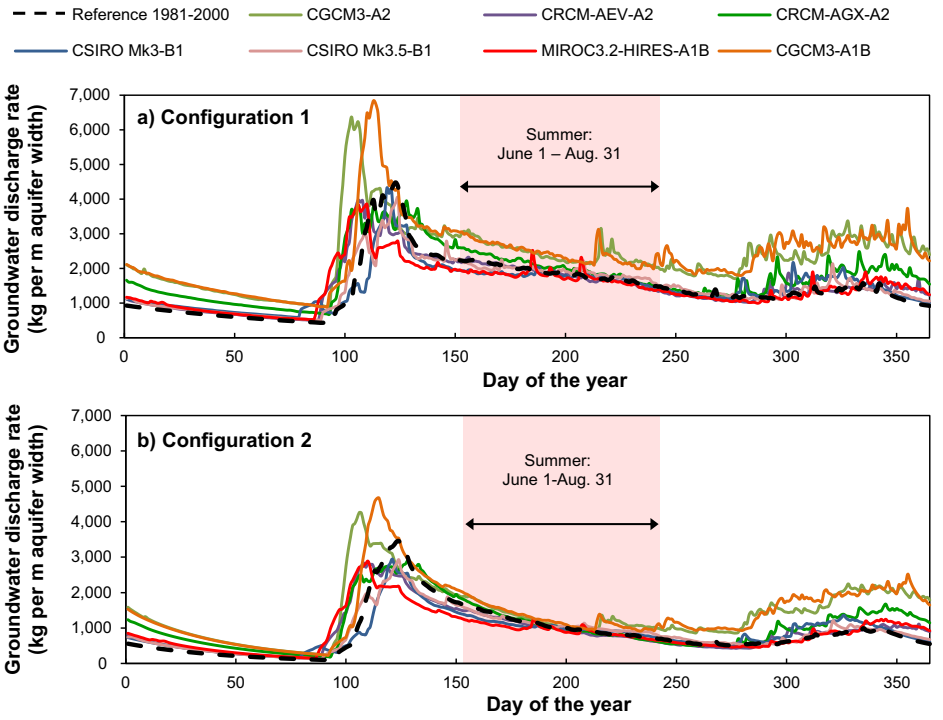

Figure 10. Simulated groundwater discharge per meter aquifer width for (a) Configuration 1 and (b) Configuration 2. Results are shown for the reference period climate (SUTRA runs R.1 and R.2) and the last 10 years of simulation (2056–2065) for SUTRA runs 1.1–7.2 (Table 2). The results are the averaged over the simulation period for each day of the year.

discharge temperature (−0.73°C and −0.53°C for Configurations 1 and 2, respectively), but all other climate scenarios result in an increase in mean annual and summer groundwater discharge temperature (Figure 6). It should be noted that actual trends in global CO_2 emissions and concentrations have exceeded emission scenario B1 projections [*Raupach et al.*, 2007], thus the CSIRO Mk3-B1 climate scenario likely underestimates future changes in climate.

The simulations also suggest that the amplitude of the seasonal groundwater temperature cycle may increase in shallow aquifers. For example, the increase in average winter groundwater discharge temperature (December–February, +1.41°C) for the MIROC3.2-HIRES-A1B scenario (Configuration 1, Figure 6a) was not as pronounced as the simulated increase in average summer groundwater discharge temperature (June–August, +3.37°C). This amplitude increase arises from the projected changes in seasonal GST, which were typically positive in the summer and negative in the winter [*Kurylyk et al.*, 2013]. These results differ from those of *Taylor and Stefan* [2009], who found that the minimum and maximum groundwater temperature would increase by approximately the same amount.

5.2. Aquifer Summer Thermal Sensitivities

Changes to the temperature of summer groundwater discharge are of particular interest to stream ecologists as this is the period most critical for the generation of thermal refugia. Figure 11 presents the simulated changes in mean annual and mean summer groundwater discharge temperature versus the changes in mean annual and mean summer AT. This information can be utilized to generally assess the thermal response of each aquifer to decadal climate change. The groundwater discharge temperature data in Figure 11 display a relatively consistent trend amongst climate scenarios (relatively high R^2 for trend lines) for each aquifer configuration; however, the slopes of the best fit lines indicate that the thermal regime of Configuration 1 is more sensitive to summer AT increases than the thermal regime of Configuration 2. This difference arises because the summer thermal regime of Configuration 1 is driven by summer GST trends, which closely follow summer AT increases. Conversely, the summer thermal regime of Configuration 2 is primarily driven by changes in mean annual GST, which were damped compared to mean annual or seasonal AT changes due to snowpack thinning or removal [*Kurylyk et al.*, 2013]. The decrease in mean annual GST

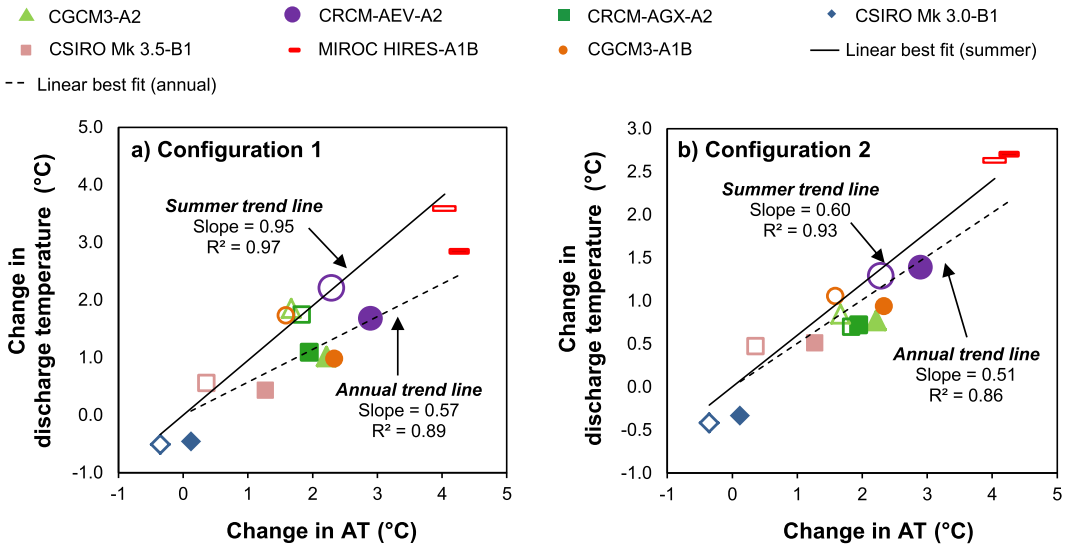

Figure 11. Simulated changes in mean annual and mean summer (1 June–31 August) groundwater discharge temperature for the last 10 years of each future period simulation (2056–2065, runs 1.1–7.2, Table 2) compared to the reference period simulation (1981–2000, runs R.1 and R.2) versus the change in mean annual and mean summer air temperature for (a) Configuration 1 and (b) Configuration 2. The mean annual results are depicted by the symbols with fill. The mean summer results are represented by symbols with the same shape and color (see legend) but with no fill. The best fit lines were constrained to have a zero intercept.

changes compared to mean annual AT changes also accounts for the higher slope through the mean summer data compared to the mean annual data (Figure 11). Configuration 2 exhibits less sensitivity to seasonal GST variability than Configuration 1 (Figure 5), thus the difference between the slopes representing mean annual and mean summer data in Figure 11 is not as pronounced for Configuration 2 (0.60–0.51=0.09) as it is for Configuration 1 (0.95–0.57=0.38). Figure 11 also indicates that, contrary to the assumptions made in other approaches [e.g., *Meisner et al.*, 1988; *Deitchman and Loheide*, 2012; *MacDonald et al.*, 2013], climate-induced changes to groundwater discharge temperature will not necessarily follow AT changes on a mean annual or seasonal basis.

Several recent studies have investigated the sensitivity of stream and river temperature to AT variations [e.g., *Bogan et al.*, 2003; *Kelleher et al.*, 2012; *Mayer*, 2012]. *Kelleher et al.* [2012] and *Mayer* [2012] specifically defined the thermal sensitivity of surface water as the slope of the surface water temperature-AT plot. These plots are typically derived from high-frequency (e.g., weekly or seasonal) AT and surface water temperature data, but can be employed to estimate the thermal response of rivers to decadal climate change [e.g., *Mayer*, 2012; *Kelleher et al.*, 2012]. The summer aquifer thermal sensitivity is herein defined as the simulated change in average summer groundwater discharge temperature for a particular climate scenario divided by the driving change in average summer AT. Note that this is a low-frequency (decadal climate change) sensitivity definition rather than the high-frequency sensitivity definition employed by surface water temperature analysts.

Table 3 indicates that the mean aquifer thermal sensitivity for Configuration 1 (1.00) is significantly higher than the mean sensitivity for Configuration 2 (0.55). The aquifer thermal sensitivities in Table 3 exceed some previously reported values for the response of stream or river temperature to climate change. For example, *Wu et al.* [2012, Table 3] simulated an average 1.37°C summer stream temperature rise in response to an average 2.81°C summer AT rise (1.37/2.81 = 0.49) for Pacific Northwest streams. Others have simulated surface water sensitivities that exceed the summer thermal sensitivity of Configuration 2 but are less than that of Configuration 1. For instance, *Morrill et al.* [2005] modeled future stream temperatures in geographically diverse locations and demonstrated that the majority of streams will exhibit increases in stream temperature of 0.6–0.8°C for each 1°C increase in AT. Thus, the site specific results shown in Table 3 suggest that the thermal regimes of certain aquifers (and thus groundwater-sourced refugia) may actually be more responsive to decadal climate change than the thermal regimes of streams and rivers. The high aquifer thermal sensitivities reported in Table 3 arise in part because aquifers do not experience free water surface

Table 3. Summer Thermal Sensitivities (STS) for Both Aquifer Configurations for 2056–2065

Climate Scenario	Δ Summer AT (°C)[a]	Configuration 1 ΔGWDT (°C)[b]	Configuration 1 STS[c]	Configuration 2 ΔGWDT (°C)[b]	Configuration 2 STS[c]
CGCM3-A2	1.67	1.85	1.11	0.85	0.51
CRCM AEV-A2	2.29	2.21	0.96	1.29	0.56
CRCM AGX-A2	1.83	1.74	0.95	0.70	0.38
CSIRO Mk 3.0-B1	−0.35	−0.51	1.45	−0.42	1.18
CSIRO Mk 3.5-B1	0.36	0.56	1.55	0.47	1.31
MIROC-HIRES	4.04	3.59	0.89	2.63	0.65
CGCM3-A1B	1.59	1.73	1.09	1.05	0.66
Average			*1.00*[d]		*0.55*[d]

[a]The change in summer AT values are with respect to the reference period (1981–2000). These deviate slightly from those reported by *Kurylyk et al*. [2013, Table 2] because the present study only considers the last 10 years of the climate scenario simulations (2056–2065).

[b]ΔGWDT = the change in summer (June–August) groundwater discharge temperature compared to the reference period (1981–2000) summer groundwater discharge temperature.

[c]STS = summer thermal sensitivity for each aquifer due to low-frequency climate variations = ΔGWDT/ΔAT.

[d]Average STS values were calculated without including the anomalous CSIRO Mk 3.0-B1 and CSIRO Mk 3.5-B1 data, as the very low summer AT changes for these two scenarios yielded unreasonably high sensitivity values.

evaporation, which cools the thermal regimes of surface water bodies during high-temperature events and thereby reduces their thermal sensitivity [*Mohseni and Stefan*, 1999].

Groundwater discharge temperature does not typically respond to high-frequency (e.g., weekly) AT variability, and thus baseflow-dominated streams tend to be characterized by lower sensitivity to weekly or daily climate variability compared to direct-flow dominated streams [*Hayashi and Rosenberry*, 2002; *Bogan et al*., 2003; *Tague et al*., 2007; *Risley et al*., 2010]. However, one should not infer from this that baseflow-dominated streams and rivers will also be less responsive to decadal climate change. We have demonstrated that aquifer thermal regimes can exhibit considerable sensitivity to low-frequency AT variations (Figure 11).

The results portrayed in Figure 11 and Table 3 indicate that there is significant variability in how climate change may influence aquifer thermal regimes. Consequently, the response of aquifers, groundwater-sourced thermal refugia, and baseflow-dominated streams to climate change may be more complex than previously thought. This merits further analysis, as the temperature of future groundwater discharge is only one of the factors controlling the future thermal regimes of baseflow-dominated streams.

5.3. Lag Between Climate Change and Groundwater Temperature Rise

Previous researchers [e.g., *Gunawardhana et al*., 2011; *Kurylyk and MacQuarrie*, 2014] have demonstrated that there is a lag between a GST increase due to climate change and its thermal impact on deeper subsurface environments. However, the thermal regime of the shallow subsurface (e.g., depth < 10 m) exhibits a very short lag in response to surficial climate change. For example, Figure 12a demonstrates that the simulated future groundwater discharge temperatures for Configurations 1 and 2 respond very quickly (<5 years) to a step change in GST due to atmospheric climate change. Furthermore, the lag would be even shorter if the boundary condition represented gradual climate change rather than the step change simulated in the present study. Configuration 2 takes $\sim$2 years longer than Configuration 1 to achieve thermal equilibrium with the new GST due to its deeper discharge point (Figure 12a). Similarly short lags for the response of groundwater temperature to surficial climate changes were obtained from the statistical analyses conducted by *Menberg et al*. [2014].

The thermal response of groundwater to climate change is often assumed to be a consideration limited to the distant future. For example, *Chu et al*. [2008] state that "the potential changes in groundwater temperatures and fish habitat may take decades or centuries to be realized." This proposition was used to justify a modeling approach that did not explicitly consider changes to groundwater conditions. The short lags shown in Figure 12a strongly demonstrate that assessments of future surface water temperature should consider relatively imminent increases in the temperature of groundwater discharge from shallow aquifers, at least in the cases where surface water thermal regimes are strongly influenced by groundwater discharge.

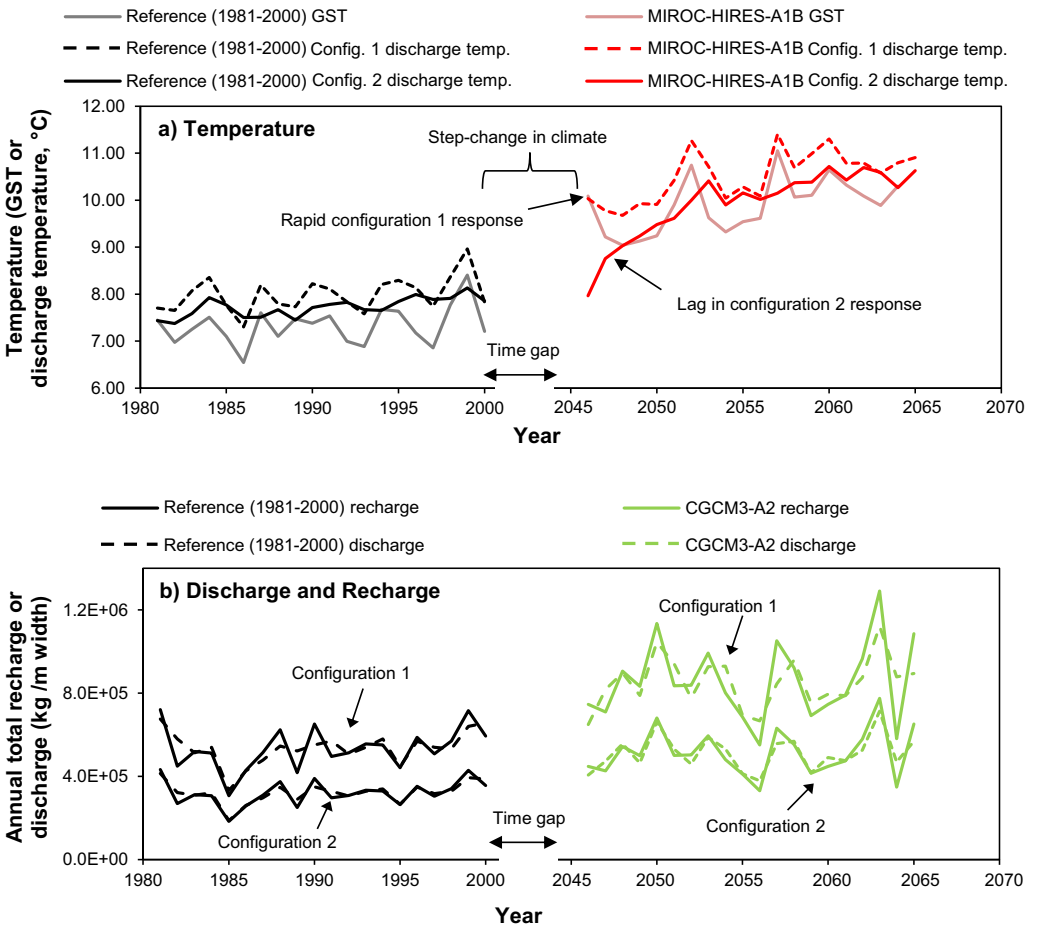

Figure 12. (a) Simulated groundwater discharge temperature for each year for the reference period (runs R.1 and R.2, Table 2) and the climate scenario exhibiting the greatest increase in groundwater discharge temperature (MIROC-HIRES-A1B, runs 6.1 and 6.2). There was a 45 year (2001–2045, inclusive) time gap between the reference period and the future period simulation. (b) (lower legend) Simulated groundwater recharge and groundwater discharge (per m aquifer width) for each year for the reference period (runs R.1 and R.2, Table 2) and the climate scenario exhibiting the greatest increase in recharge/discharge (CGCM3-A2, runs 1.1 and 1.2).

5.4. Subsurface Thermal Influence of Advection and Pore Water Phase Change

The reference period simulations performed with and without groundwater flow (Figure 7) indicate that advective influences can be significant (max difference between series = 3.1°C). In general, models ignoring advection can underpredict summer groundwater discharge temperature and thus overpredict the ability of that discharge point to provide thermal refuge. This illustrates the limitations of employing a simple conduction-only model to investigate the response of groundwater discharge to climate change or seasonal temperature variation. A more detailed investigation of the internal aquifer energy balance and the relative roles of conduction and advection is included in supporting information (text02 and fs04).

Figure 8 indicates that the influence of pore water phase change on groundwater discharge temperature can be significant in a given year, but it tends to be minimal in this catchment when averaged over the 20 year simulation period. The thermal influence of the dynamic freeze-thaw process is more apparent in shallow subsurface temperature profiles (e.g., 1 or 2 m depth) recorded halfway up the hillslope (supporting information Figure fs03). In general, not accounting for the latent energy released during freezing yields shallow subsurface temperatures that are too low during the onset of freezing in the late fall-early winter. Conversely, not accounting for the latent heat absorbed during thawing will typically yield shallow subsurface temperatures that are too high during the late winter-early spring thaw. At higher latitudes or altitudes, the frost penetration depth increases, and latent heat effects influence thermal regimes at greater depths [*Zhang et al.*, 2008; *Woo*, 2012]. Latent energy effects due to pore water phase change are also more apparent in soils with higher porosity and moisture retention properties, such as peat [*McKenzie et al.*, 2007].

Thus, the influence of pore water phase change on the temperature of groundwater discharge would be even more evident in colder climates or for different soils than those considered in the present study. The simulations presented in this study help elucidate the complex thermal dynamic of shallow aquifers and thereby inform researchers of the limitations arising from employing simplified models.

5.5. Impact of Climate Change on Groundwater Discharge Rates

5.5.1. Impact of Climate Change on the Magnitude and Timing of Mean Annual and Maximum Groundwater Discharge

The hydraulic conditions of shallow aquifers may also respond rapidly to atmospheric climate change. Figure 12b presents the annual total discharge and recharge rates for the reference period and the climate scenario exhibiting the greatest increase in recharge and discharge. Clearly, both aquifer configurations adjust quickly to the surface hydraulic perturbations. The step increase in groundwater recharge due to climate change results in an approximately corresponding step increase in groundwater discharge within 1 year. This rapid response in annual groundwater discharge due to changes in annual groundwater recharge is expected given that these shallow unconfined aquifers also responded quickly to intra-annual recharge variability (Figure 9). Figure 12b also indicates that total groundwater discharge will not exactly equal total groundwater recharge in a given year due to aquifer storage capabilities.

Figure 10 presents the simulated changes in groundwater discharge for each climate scenario throughout the year. Despite similarities noted in the results, there are also discernible differences between the simulated groundwater discharge series for each climate scenario. For example, average annual discharge rates increase significantly for the CGCM3-A2 and CGCM3-A1B scenarios compared to the reference period simulation (increase of mean annual groundwater discharge $\sim$60% for both configurations). These increases in discharge are not surprising given the significant projected increases in precipitation (50%, Figure 3a) and recharge (58%, Figure 3b) for these two climate scenarios. Changes to groundwater discharge on this order can significantly alter the total river discharge of baseflow-dominated rivers, and total river discharge has been shown to influence the thermal response of rivers to warming climates [see *van Vliet et al*., 2011; *Deitchman and Loheide*, 2012]. Thus, changes to groundwater discharge may need to be accounted for when modeling future riverine thermal regimes. Figure 10 also indicates that the peak discharge rates for the CGCM3-A1B simulation increase by 53% for Configuration 1 and only 35% for Configuration 2. These differences arise because Configuration 2, which has a deeper discharge point than Configuration 1, attenuates the temporal variability in recharge and consequent discharge more than Configuration 1.

As Figure 10 illustrates, the average timing of the maximum discharge rate is shifted earlier in the year for most of the climate scenarios due to the earlier snowmelt simulated in HELP3 [*Kurylyk and MacQuarrie*, 2013]. These shifts are similar for Configuration 1 (range = -17 to $+1$ days, negative implies earlier discharge event) and Configuration 2 (range = -17 to $+4$ days). As indicated by the MIROC3.2-HIRES-A1B simulation (Figure 10), a shift in the timing of the major discharge event may cause shallow, unconfined aquifers to be more fully drained by early summer and thereby reduce early summer groundwater discharge rates.

5.5.2. Impact of Climate Change on the Magnitude of Summer Groundwater Discharge

Figure 10 indicates that future summer groundwater discharge rates simulated for Configuration 1 deviate more from the reference period simulation than summer groundwater discharge rates simulated for Configuration 2. For example, simulated changes in average summer groundwater discharge rates for Configuration 1 range from -6% to $+31$% with a mean of $+8.4$%, while simulated changes in average summer discharge for Configuration 2 range from -12% to $+19$% with a mean of $+2.1$%. The maximum simulated increases in summer groundwater discharge for both aquifers are significant ($+31$% and $+19$% for Configurations 1 and 2), but they are damped with respect to the increase in annual precipitation for this climate scenario ($+50$%, Figure 3A). This damping arises because much of the simulated increase in annual precipitation for this particular climate scenario (CGCM3-A1B) occurs during the winter months. This precipitation temporarily accumulates in the form of snow and recharges the aquifer in the spring. The extra aquifer storage is predominantly discharged from the aquifer prior to the summer months. Additionally, due to the projected increases in summer AT for the CGCM3-A1B scenario, simulated evapotranspiration rates increase and reduce the soil moisture available for recharge [*Kurylyk and MacQuarrie*, 2013]. In general, the physical

dimensions of Configuration 2 cause it to be less hydraulically sensitive to increases in summer precipitation than Configuration 1.

5.6. Implications for Groundwater-Sourced Salmonid Refugia

The relationship between climate change, rising river water temperatures, and the loss of future cold water fish habitat has been well studied [e.g., *Chu et al.*, 2005; *Isaak et al.*, 2012; *Jonsson and Jonsson*, 2009; *Wu et al.*, 2012, and references therein]. Given the importance of groundwater-sourced thermal refugia in warming riverine ecosystems, there remains a surprising paucity of studies investigating physical processes that generate refugia and their vulnerability to climate change. The results from the present study can be utilized to perform a preliminary analysis of the ecological implications of changes to the thermal and hydraulic regimes of unconfined, alluvial aquifers.

The results presented in Figure 10 indicate that summer groundwater discharge rates will increase or be relatively constant for most of the climate scenarios. However, for the MIROC3.2-HIRES-A1B climate scenario, the average magnitude of the simulated summer discharge for Configuration 2 decreases 12% relative to the reference period simulation (Figure 10b). Such a reduction in groundwater flow at concentrated points of discharge (Figure 1c) could reduce the spatial extent of groundwater-sourced thermal refugia, which can already be overpopulated during high-temperature events.

A simple probabilistic approach can yield a first-order estimate of the ecological impacts of the aquifer warming depicted in Figure 11. Juvenile Atlantic salmon do not typically aggregate within thermal refugia in the Little Southwest Miramichi River (LSW) and surrounding river systems until ambient river temperatures exceed 22°C [*Cunjak et al.*, 2005]. Surface water surveys conducted in the cold water tributary considered in the present study (Otter Brook, Figure 1 and Configuration 1, Figure 4a) indicate that once groundwater discharges into the tributary it will experience significant downstream warming due to thermal mixing with warmer surface water and exposure to solar radiation. This warming can be on the order of 4°C in regions of significant groundwater discharge to the tributary. In the case of 4°C intermediate warming, groundwater discharge temperature to the tributary should not exceed 18°C (22°C–4°C), or the refuge at the confluence with the LSW will not provide optimal thermal conditions for stressed salmonids. This target temperature (18°C) was selected to examine the probability that the aquifer discharging to the tributary (Configuration 1) could continue to provide suitable thermal habitat under the most extreme warming scenario (MIROC3.2-HIRES-A1B, Figure 3).

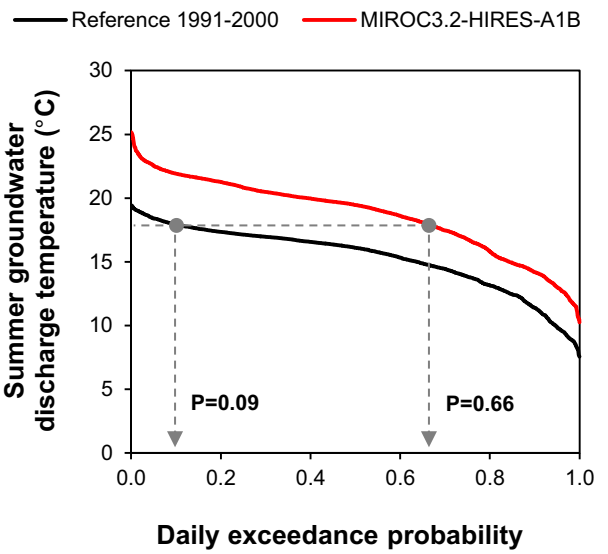

Figure 13. Summer (1 June–31 August) groundwater discharge temperature from Configuration 1 for the recent reference period (1991–2000, run R.1, Table 2) and MIROC3.2-HIRES-A1B (2056–2065, run 6.1) simulations versus the probability that the temperature would be exceeded on any given day in the summer. The daily exceedance probabilities for a groundwater discharge temperature of 18°C are shown.

The simulated mean daily summer groundwater discharge temperatures for the reference period (run R.1) and the warmest climate scenario (run 6.1) were ranked and assigned a probability in accordance with the Weibull ranking method [*McCuen*, 1993]. Figure 13 indicates that the reference period probability of exceeding the 18°C target temperature on any given day in the summer is 9%, but this probability increases to 66% in the warming climate. Thus, this shallow, unconfined aquifer may not continue to provide optimal thermal refuge for the majority of the summer under the most extreme warming scenario. Note that this simplistic approach assumes that the future change in the water temperature of Otter Brook, which is baseflow-dominated, will correspond to the change in the groundwater discharge temperature. The actual future water temperature increases in Otter Brook may also be

influenced by other factors, including changes to future air temperature and precipitation regimes and land cover changes. A similar analysis conducted for Configuration 2 (results not shown), which discharges directly into the LSW and thus experiences no intermediate warming, indicates that the aquifer will continue to consistently provide a small thermal refuge under each of the climate scenarios considered in this study. These analyses should not be used to make definitive predictions regarding the future state of the Otter Brook or seep thermal refugia (Figure 1), but they do provide insight into how varying aquifer morphologies and refugia characteristics (e.g., direct or indirect groundwater discharge) may influence their thermal response to climate change.

5.7. Limitations

The modeling approach used in the present study (Figures 2 and 4) employed several simplifying assumptions. First, the recharge output from HELP3 and the GST output from ForHyM2 were expressed as point conditions. Thus, the surface conditions were assumed to be thermally and hydraulically uniform, which is a reasonable assumption given the small size (<10 km^2) and low topographic relief of the catchments studied. Second, the recharging water was assumed to be in thermal equilibrium with GST. The temperature of precipitation and infiltration is influenced by the thermal regime of the lower atmosphere and may deviate from GST. Third, the aquifer thermal and hydraulic conductivities were assumed to depend only on the moisture conditions or direction of groundwater flow, but saturated subsurface environments are characterized by heterogeneity in their thermal and hydraulic properties [*Domenico and Schwartz*, 1990]. Despite these limitations, the simulation results provide valuable insights into the hydraulic and thermal sensitivities of unconfined aquifers to climate change and the associated impacts to groundwater-sourced fish habitat.

6. Conclusions

The sensitivity of groundwater discharge to climate change was investigated by utilizing downscaled climate scenarios to drive surface and subsurface simulations in idealized catchments/aquifers whose properties were derived from field observations of aquifers generating thermal refugia. To our knowledge, this research is the first to utilize downscaled climate scenarios to form the boundary conditions for multidimensional simulations of groundwater flow and heat transport.

Five main conclusions can be extracted from the results and discussion.

1. The thermal regimes of thin, shallow aquifers are not resilient to decadal climate change. In certain instances, the simulated aquifer thermal sensitivities to climate change (average values of 1.0 for Configuration 1 and 0.55 for Configuration 2) exceed those previously reported for rivers and streams. Thus, high groundwater discharge rates should not necessarily be presumed to provide a buffer to future climate change. Furthermore, changes to groundwater discharge temperature will not necessarily closely track changes to AT in seasonally snow-covered catchments due to the complex dynamics of snowpack evolution.

2. The lag between a rise in AT and the thermal response of shallow groundwater may be overestimated in previous studies. Groundwater discharge from the aquifers simulated in the present study reached thermal equilibrium with changing climatic conditions in <5 years. Therefore, groundwater temperature evolution due to climate change may need to be considered in deterministic models of surface water thermal regimes.

3. In catchments experiencing seasonal freeze-thaw, daily groundwater discharge temperature can be impacted by advection, conduction, and the dynamic freeze-thaw process. Thus, future research investigating the sensitivity of shallow groundwater temperature to climate change should not employ simplified conduction models unless they have been shown to perform well for the aquifer being considered.

4. The timing and magnitude of groundwater discharge may also respond quickly to changes in precipitation and groundwater recharge. Projected changes in the magnitude of mean annual recharge and discharge range from $\sim-6\%$ to $+60\%$ compared to the reference period recharge. The peak groundwater discharge event associated with snowmelt is generally shifted earlier in the year (up to 17 days). Discharge from these aquifers is sensitive to changes in groundwater recharge on temporal scales ranging from

weekly to decadal. These changes to groundwater discharge magnitude and timing will influence the thermal regimes of baseflow-dominated streams.

5. The ability of groundwater discharge to continue to produce biologically significant thermal refugia in a warming climate depends strongly on the aquifer configuration, refuge characteristics (indirect or direct groundwater discharge), and the particular climate scenario employed. Furthermore, we have demonstrated that the probability of exceeding critical temperature thresholds within certain thermal refugia will likely increase in the coming decades. This is alarming given the presumed increased reliance on thermal refugia in a warming climate. Although these results are site specific, they should challenge researchers to reconsider their preconceptions regarding the future thermal states of groundwater dependent ecosystems.

Although shallow groundwater temperature will respond to a gradually warming climate, groundwater discharge will continue to buffer river temperatures throughout the summer months, particularly during extreme events. Consequently, the ecological significance of groundwater-surface water interactions should be considered in future comprehensive land use management strategies [e.g., *Saltveit and Braband*, 2013; *Nichols et al*., 2013]. Catchments overlying unconfined aquifers generating thermal refugia should be protected from anthropogenic activity such as deforestation and groundwater and aggregate extraction, as these processes have been shown to increase shallow groundwater temperature [*Alexander et al*., 2003; *Moore et al*., 2005; *Markle and Schincariol*, 2007; *Risley et al*., 2010; *Barlow and Leake*, 2012]. The results from the present study further indicate that the thermal regimes of certain unconfined aquifers will be more resilient to climate change than others. Thus, our results suggest that knowledge of local hydrogeology will assist in prioritizing appropriate catchments for the preservation of future thermal refugia. Further research is required to provide additional information on the preservation and enhancement of groundwater-sourced thermal refugia.

Acknowledgments

We appreciate the constructive comments offered by the Associate Editor and two anonymous reviewers. J. McKenzie of McGill University also provided helpful comments on this paper. The climate data and information provided by D. Huard (Ouranos) and D. I. Jeong, A. Daigle and A. St-Hilaire (Université du Québec Institut National de la Recherche Scientifique) are gratefully acknowledged. A. Provost of the U.S. Geological Survey and J. McKenzie of McGill University provided valuable advice and assistance with SUTRA. T. Linnansaari (Canadian Rivers Institute) contributed information regarding fish aggregations within the Little Southwest Miramichi River. This research has been funded by the Canada Research Chairs Program and an NSERC Collaborative Research and Development Grant. B. L. Kurylyk was also funded by NSERC postgraduate scholarships (Julie Payette PGS and CGSD3) and an O'Brien Fellowship. This paper is contribution 125 of the Catamaran Brook Habitat Research Project.

References

Alexander, M. D., K. T. B. MacQuarrie, D. Caissie, and K. E. Butler (2003), The thermal regime of shallow groundwater and a small Atlantic salmon stream bordering a clearcut with a forested streamside buffer, *Proceedings of Annual Conference of the Canadian Society for Civil Engineering, 1899–1908*, Moncton, New Brunswick, Canada.

Allard, S. (2008), Otter Brook granular aggregate deposit (NTS 21 J/16), north-central New Brunswick: Geotechnical data and ground-penetrating radar survey results, *Open File Rep. 2008-10*, 32 pp., New Brunswick Dep. of Nat. Resour., Miner. Policy and Plann. Div., Fredericton, N. B.

Allen, D. M., A. J. Cannon, M. W. Toews, and J. Scibek (2010), Variability in simulated recharge using different GCMs, *Water Resour. Res.*, *46*, W00F03, doi:10.1029/2009WR008932.

Balland, V., J. Bhatti, R. Errington, M. Castonguay, and P. A. Arp (2006), Modeling snowpack and soil temperature and moisture conditions in a jack pine, black spruce and aspen forest stand in central Saskatchewan (BOREAS SSA), *Can. J. Soil Sci.*, *86*(2), 203–217.

Barlow, P. M., and S. A. Leake (2012), Streamflow depletion by wells—Understanding and managing the effects of groundwater pumping on streamflow, *U.S. Geol. Surv. Circ.*, *1376*, 84 p., U.S. Geol. Surv., Reston, Va.

Befus, K. M., M. B. Cardenas, D. V. Erler, I. R. Santos, and B. D. Eyre (2013), Heat transport dynamics at a sandy intertidal zone, *Water Resour. Res.*, *49*, 3770–3786, doi:10.1002/wrcr.20325.

Bense, V. F., G. Ferguson, and H. Kooi (2009), Evolution of shallow groundwater flow systems in areas of degrading permafrost, *Geophys. Res. Lett.*, *36*, L22401, doi:10.1029/2009GL039225.

Bilby, R. E. (1984), Characteristics and frequency of cool-water areas in a western Washington stream, *J. Freshwater Ecol.*, *2*(6), 593–602, doi:10.1080/02705060.1984.9664642.

Biro, P. A. (1998), Staying cool: Behavioral thermoregulation during summer by young-of-year brook trout in a lake, *Trans. Am. Fish. Soc.*, *127*(2), 212–222, doi:10.1577/1548–8659(1998)127<0212:SCBTDS>2.0.CO;2.

Boe, J., L. Terray, F. Habets, and E. Martin (2007), Statistical and dynamical downscaling of the Seine basin climate for hydro-meteorological studies, *Int. J. Climatol.*, *27*(12), 1643–1655, doi:10.1002/joc.1602.

Bogan, T., O. Mohseni, and H. G. Stefan (2003), Stream temperature-equilibrium temperature relationship, *Water Resour. Res.*, *39*(9), 1245, doi:10.1029/2003WR002034.

Bonan, G. (2008), *Ecological Climatology*, Cambridge Univ. Press, Cambridge, U. K.

Breau, C., R. A. Cunjak, and G. Bremset (2007), Age-specific aggregation of wild juvenile Atlantic salmon *Salmo salar* at cool water sources during high temperature events, *J. Fish Biol.*, *71*(4), 1179–1191, doi:10.1111/j.1095-8649.2007.01591.x.

Breau, C., R. A. Cunjak, and S. J. Peake (2011), Behaviour during elevated water temperatures: Can physiology explain movement of juvenile Atlantic salmon to cool water?, *J. Anim. Ecol.*, *80*(4), 844–853, doi:10.1111/j.1365-2656.2011.01828.x.

Brewer, S. K. (2013), Groundwater influences on the distribution and abundance of riverine smallmouth bass, *Micropterus dolomieu*, in pasture landscapes of the midwestern USA, *River Res. Appl.*, *29*(3), 269–278, doi:10.1002/rra.1595.

Briggs, M. A., E. B. Voytek, F. D. Day-Lewis, D. O. Rosenberry, and J. W. Lane (2013), Understanding water column and streambed thermal refugia for endangered mussels in the Delaware River, *Environ. Sci. Technol.*, *47*(20), 11,423–11,431, doi:10.1021/es4018893.

Bunt, C. M., N. E. Mandrak, D. C. Eddy, S. A. Choo-Wing, T. G. Heiman, and E. Taylor (2013), Habitat utilization, movement and use of groundwater seepages by larval and juvenile Black Redhorse, *Moxostoma duquesnei, Environ. Biol. Fishes*, *96*(10–11), 1281–1287, doi:10.1007/s10641-013-0113-y.

Caissie, D. (2006), The thermal regime of rivers: A review, *Freshwater Biol.*, *51*(8), 1389–1406, doi:10.1111/j.1365-2427.2006.01597.x.

Caissie, D., M. G. Satish, and N. El-Jabi (2007), Predicting water temperatures using a deterministic model: Application on Miramichi River catchments (New Brunswick, Canada), *J. Hydrol.*, *336*(3–4), 303–315, doi:10.1016/j.jhydrol.2007.01.008.

Chen, H., C. Xu, and S. Guo (2012), Comparison and evaluation of multiple GCMs, statistical downscaling and hydrological models in the study of climate change impacts on runoff, *J. Hydrol.*, *434*, 36–45, doi:10.1016/j.jhydrol.2012.02.040.

Chu, C., N. E. Mandrak, and C. K. Minns (2005), Potential impacts of climate change on the distributions of several common and rare freshwater fishes in Canada, *Diversity Distrib.*, *11*(4), 299–310, doi:10.1111/j.1366-9516.2005.00153.x.

Chu, C., N. E. Jones, N. E. Mandrak, A. R. Piggott, and C. K. Minns (2008), The influence of air temperature, groundwater discharge, and climate change on the thermal diversity of stream fishes in southern Ontario watersheds, *Can. J. Fish. Aquat. Sci.*, *65*(2), 297–308, doi:10.1139/F08-007.

Crosbie, R. S., W. R. Dawes, S. P. Charles, F. S. Mpelasoka, S. Aryal, O. Barron, and G. K. Summerell (2011), Differences in future recharge estimates due to GCMs, downscaling methods and hydrological models, *Geophys. Res. Lett.*, *38*, L11406, doi:10.1029/2011GL047657.

Cunjak, R. A., D. Caissie, N. El-Jabi, P. Hardie, J. H. Conlon, T. L. Pollock, D. J. Giberson, and S. Komadina-Douthwright (1993), The Catamaran Brook (New Brunswick) habitat research project: Biological, physical, and chemical conditions (1990–1992), *Can. Tech. Rep. Fish. Aquat. Sci.* 1914, 81 pp., Dep. of Fish. and Ocean, Moncton, New Brunswick, Canada.

Cunjak, R. A., J. M. Roussel, M. Gray, J. Dietrich, D. Cartwright, K. Munkittrick, and T. Jardine (2005), Using stable isotope analysis with telemetry or mark-recapture data to identify fish movement and foraging, *Oecologia*, *144*(4), 636–646, doi:10.1007/s00442-005-0101-9.

Cunjak, R. A., T. Linnansaari, and D. Caissie (2013), The complex interaction of ecology and hydrology in a small catchment: A salmon's perspective, *Hydrol. Processes*, *27*(S1), 741–749, doi:10.1002/hyp.9640.

de Elia, R., D. Caya, H. Cote, A. Frigon, S. Biner, M. Giguere, D. Paquin, R. Harvey, and D. Plummer (2008), Evaluation of uncertainties in the CRCM-simulated North American climate, *Clim. Dyn.*, *30*(2–3), 113–132, doi:10.1007/s00382-007-0288-z.

Deitchman, R., and S. P. Loheide (2012), Sensitivity of thermal habitat of a trout stream to potential climate change, Wisconsin, United States, *J. Am. Water Resour. Assoc.*, *48*(6), 1091–1103, doi:10.1111/j.1752-1688.2012.00673.x.

Domenico, P. A., and F. W. Schwartz (1990), *Physical and Chemical Hydrogeology*, John Wiley, New York.

Dugdale, S. J., N. E. Bergeron, and A. St-Hilarie (2013), Temporal variability of thermal refuges and water temperature patterns in an Atlantic salmon river, *Remote Sens. Environ.*, *136*, 358–373, doi:10.1016/j.rse.2013.05.018.

Ebersole, J. L., W. J. Liss, and C. A. Frissell (2003), Thermal heterogeneity, stream channel morphology, and salmonid abundance in northeastern Oregon streams, *Can. J. Fish. Aquat. Sci.*, *60*(10), 1266–1280, doi:10.1139/F03-107.

Environment Canada (EC) (2011), *Environment Canada Adjusted and Homogenized Daily Canadian Climate Data*. [Available at http://www.ec.gc.ca/dccha-ahccd/default.asp?lang=En&n=B1F8423A-1.], Environment Canada, Ottawa, Ontario, Canada.

Environment Canada (EC) (2013), *Environment Canada Historical Weather Database for Miramichi RCS*. [Available at http://www.climate.weatheroffice.gc.ca/climateData/dailydata_e.html?Prov=XX&timeframe=2&StationID=10808&Day=1&Month=1&Year=2010&cmdB1=Go.], Environment Canada, Ottawa, Ontario, Canada.

Frampton, A., S. L. Painter, and G. Destouni (2013), Permafrost degradation and subsurface-flow changes caused by surface warming trends, *Hydrogeol. J.*, *21*(1), 271–280, doi:10.1007/s10040-012-0938-z.

Goniea, T. M., M. L. Keefer, T. C. Bjornn, C. A. Peery, D. H. Bennett, and L. C. Stuehrenberg (2006), Behavioral thermoregulation and slowed migration by adult fall Chinook salmon in response to high Columbia River water temperature, *Trans. Am. Fish. Soc*, *135*(2), 334–346, doi:10.1242/jeb.020065.

Green, T. R., M. Taniguchi, H. Kooi, J. J. Gurdak, D. M. Allen, K. M. Hiscock, H. Treidel, and A. Aureli (2011), Beneath the surface of global change: Impacts of climate change on groundwater, *J. Hydrol.*, *405*(3–4), 532–560, doi:10.1016/j.jhydrol.2011.05.002.

Gunawardhana, L. N., S. Kazama, and S. Kawagoe (2011), Impact of urbanization and climate change on aquifer thermal regimes, *Water Resour. Manage.*, *25*(13), 3247–3276, doi:10.1007/s11269-011-9854-6.

Hayashi, M., and D. O. Rosenberry (2002), Effects of ground water exchange on the hydrology and ecology of surface water, *Ground Water*, *40*(3), 309–316, doi:10.1111/j.1745-6584.2002.tb02659.x.

Hazen, A. (1911), Discussions of 'Dams on sand foundations' by A.C. Koenig, *Trans. Am. Soc. Civ. Eng.*, *73*, 199–203.

Huard, D. (2011), *Climate Change Scenarios: Thermal Refuge for Salmonids*, Ouranos Consortium on Reg. Climatol. and Adaption to Clim. Change, Quebec, Canada.

Isaak, D. J., S. Wollrab, D. Horan, G. Chandler (2012), Climate change effects on stream and river temperatures across the northwest US from 1980-2009 and implications for salmonid fishes, *Clim. Change*, *113*(2), 499–524, doi:10.1007/s10584-011-0326-z.

Jeong, D. I., A. St-Hilaire, T. B. M. J. Ouarda, and P. Gachon (2012a), Multisite statistical downscaling model for daily precipitation combined by multivariate multiple linear regression and stochastic weather generator, *Clim. Change*, *114*(3–4), 567–591, doi:10.1007/s10584-012-0451-3.

Jeong, D. I., A. St-Hilaire, T. B. M. J. Ouarda, and P. Gachon (2012b), A multivariate multi-site statistical downscaling model for daily maximum and minimum temperatures, *Clim. Res.*, *54*(2), 129–148, doi:10.3354/cr01106.

Jones, L. A., C. C. Muhlfeld, L. A. Marshall, B. L. McGlynn, and J. L. Kershner (2013), Estimating thermal regimes of bull trout and assessing the potential effects of climate warming on critical habitats, *River Res. Appl.*, *30*, 204–216, doi:10.1002/rra.2638.

Jonsson, B., and N. Jonsson (2009), A review of the likely effects of climate change on anadromous Atlantic salmon *Salmo salar* and brown trout *Salmo trutta*, with particular reference to water temperature and flow, *J. Fish Biol.*, *75*(10), 2381–2447, doi:10.1111/j.1095-8649.2009.02380.x.

Kanno, Y., J. C. Vokoun, and B. H. Letcher (2013), Paired stream-air temperature measurements reveal fine-scale thermal heterogeneity within headwater brook trout stream networks, *River Res. Appl.*, doi:10.1002/rra.2677.

Kelleher, C., T. Wagener, M. Gooseff, B. McGlynn, K. McGuire, and L. Marshall (2012), Investigating controls on the thermal sensitivity of Pennsylvania streams, *Hydrol. Processes*, *26*(5), 771–785, doi:10.1002/hyp.8186.

Kurylyk, B. L., and K. T. B. MacQuarrie (2013), The uncertainty associated with estimating future groundwater recharge: A summary of recent research and an example from a small unconfined aquifer in a northern climate, *J. Hydrol.*, *492*(7), 244–253, doi:10.1016/j.jhydrol.2013.03.043.

Kurylyk, B. L., and K. T. B. MacQuarrie (2014), A new analytical solution for assessing projected climate change impacts on subsurface temperature, *Hydrol. Processes*, *28*(7), 3161–3172, doi:10.1002/hyp.9861.

Kurylyk, B. L., and K. Watanabe (2013), The mathematical representation of freezing and thawing processes in variably-saturated, non-deformable soils, *Adv. Water Resour.*, *60*, 160–177, doi:10.1016/j.advwatres.2013.07.016.

Kurylyk, B. L., C. P. A. Bourque, and K. T. B. MacQuarrie (2013), Potential surface temperature and shallow groundwater temperature response to climate change: An example from a small forested catchment in east-central New Brunswick (Canada), *Hydrol. Earth Syst. Sci.*, *17*, 2701–2716, doi:10.5194/hess-17-2701-2013.

MacDonald, R. J., S. Boon, J. M. Byrne, M. D. Robinson, and J. B. Rasmussen (2013), Potential future climate effects on mountain hydrology, stream temperature, and native salmonid life-history, *Can J. Fish. Aquat. Sci.*, *71*(2), 189–202, doi:10.1139/cjfas-2013-0221.
Markle, J. M., and R. A. Schincariol (2007), Thermal plume transport from sand and gravel pits—Potential thermal impacts on cool water streams, *J. Hydrol.*, *338*(3–4), 174–195, doi:10.1016/j.jhydrol.2007.02.031.
Mayer, T. D. (2012), Controls of summer stream temperature in the Pacific Northwest, *J. Hydrol.*, *475*, 323–335, doi:10.1016/j.jhydrol.2012.10.012.
McCuen, R. H. (1993), *Microcomputer Applications in Statistical Hydrology*, Prentice Hall, Englewood Cliffs, N. J.
McKenzie, J. M., and C. I. Voss (2013), Permafrost thaw in a nested groundwater-flow system, *Hydrogeol. J.*, *21*(1), 299–316, doi:10.1007/s10040-012-0942-3.
McKenzie, J. M., C. I. Voss, and D. I. Siegel (2007), Groundwater flow with energy transport and water–ice phase change: Numerical simulations, benchmarks, and application to freezing in peat bogs, *Adv. Water Resour.*, *30*(4), 966–983, doi:10.1016/j.advwatres.2006.08.008.
Meehl, G. A., et al. (2007a), Global climate projections, in *Climate Change 2007: The Physical Science Basis. Contributions of Working Group 1 to the Fourth Assessment Report of the Intergovernmental Panel on Climate Change*, edited by S. Solomon et al., pp. 747–845, Cambridge Univ. Press, Cambridge, U. K.
Meehl, G. A., C. Covey, T. Delworth, M. Latif, B. McAvaney, J. F. B. Mitchell, R. J. Stouffer, and K. E. Taylor (2007b), The WCRP CMIP3 multimodel dataset—A new era in climate change research, *Bull. Am. Meteorol. Soc.*, *88*(9), 1383–1394, doi:10.1175/BAMS-88-9-1383.
Meisner, J. D., J. S. Rosenfeld, and H. A. Regier (1988), The role of groundwater in the impact of climate warming on stream salmonines, *Fisheries*, *13*(3), 2–8, doi:10.1577/1548–8446(1988)013<0002:TROGIT>2.0.CO;2.
Menberg, K., P. Blum, B. L. Kurylyk, and P. Bayer (2014), Observed groundwater temperature response to recent climate change, *Hydrol. Earth Syst. Sci. Discuss.*, *11*, 3637–3673, doi:10.5194/hessd-11-3637-2014.
Mohseni, O., and H. G. Stefan (1999), Stream temperature air temperature relationship: A physical interpretation, *J. Hydrol.*, *218*(3–4), 128–141, doi:10.1016/S0022-1694(99)00034-7.
Mohseni, O., H. G. Stefan, and J. G. Eaton (2003), Global warming and potential changes in fish habitat in U.S. streams, *Clim. Change*, *59*(3), 389–409, doi:10.1023/A:1024847723344.
Monk, W. A., N. M. Wilbur, R. A. Curry, R. Gagnon, and R. N. Faux (2013), Linking landscape variables to cold water refugia in rivers, *J. Environ. Manage.*, *118*, 1701–1776, doi:10.1016/j.jenvman.2012.12.024.
Moore, R. D., P. Sutherland, T. Gomi, and A. Dhakal (2005), Thermal regime of a headwater stream within a clear-cut, coastal British Columbia, Canada, *Hydrol. Processes*, *19*(13), 2591–2608.
Moore, R. D., M. Nelitz, and E. Parkinson (2013), Empirical modelling of maximum weekly average stream temperature in British Columbia, Canada, to support assessment of fish habitat suitability, *Can. Water Res. J.*, *38*(2), 135–147, doi:10.1080/07011784.2013.794992.
Morrill, J., R. Bales, and M. Conklin (2005), Estimating stream temperature from air temperature: Implications for future water quality, *J. Environ. Eng.*, *131*(1), 139–146, doi:10.1061/(ASCE)0733-9372(2005)131:1(139).
New Brunswick Aquatic Data Warehouse (NBADW) (2011), *New Brunswick Aquatic Data Warehouse*. [Available at http://www.unb.ca/research/institutes/cri/nbaquatic/index.html.], Canadian Rivers Institute, Fredericton, NB, Canada.
Nichols, A. L., A. D. Willis, C. A. Jeffres, and M. L. Deas (2013), Water temperature patterns below large groundwater springs: Management implications for Coho Salmon in the Shasta River, California, *River Res. Appl.*, doi:10.1002/rra.2655.
Nielsen, J. L., T. E. Lisle, and V. Ozaki (1994), Thermally stratified pools and their use by steelhead in northern California streams, *Trans. Am. Fish. Soc.*, *123*(4), 613–626.
Olsen, D. A., and R. G. Young (2009), Significance of river-aquifer interactions for reach-scale thermal patterns and trout growth potential in the Motueka River, New Zealand, *Hydrogeol. J.*, *17*(1), 175–183, doi:10.1007/s10040-008-0364-4.
Painter, S. (2011), Three-phase numerical model of water migration in partially frozen geological media: Model formulation, validation, and applications, *Comput. Geosci.*, *15*(1), 69–85, doi:10.1007/s10596-010-9197-z.
Raupach, M. R., G. Marland, P. Ciais, C. Le Quere, J. G. Canadell, G. Klepper, and C. B. Field (2007), Global and regional drivers of accelerating CO_2 emissions, *Proc. Natl. Acad. Sci. U. S. A.*, *104*(24), 10,288–10,293, doi:10.1073/pnas.0700609104.
Risley, J. C., J. Constantz, H. Essaid, and S. Rounds (2010), Effects of upstream dams versus groundwater pumping on stream temperature under varying climate conditions, *Water Resour. Res.*, *46*, W06517, doi:10.1029/2009WR008587.
Saltveit, S. J., and Å. Brabrand (2013), Incubation, hatching and survival of eggs of Atlantic salmon (*Salmo salar*) in spawning redds influenced by groundwater, *Limnologica*, *43*(5), 325–331, doi:10.1016/j.limno.2013.05.009.
Sanford, W. (2002), Recharge and groundwater models: An overview, *Hydrogeol. J.*, *10*(1), 110–120, doi:10.1007/s10040-001-0173-5.
Schroeder, P. R., T. S. Dozier, P. A. Zappi, B. M. McEnroe, J. W. Sjostrom, and R. Peyton (1994), The hydrologic evaluation of landfill performance (HELP) model. Engineering Documentation for version 3, *Rep. EPA/600/R-94/168b*, U.S. Environ. Prot. Agency, Off. of Res. and Dev., Washington, D. C.
Story, A., R. D. Moore, and J. S. Macdonald (2003), Stream temperatures in two shaded reaches below cutblocks and logging roads: Downstream cooling linked to subsurface hydrology, *Can. J. For. Res.*, *33*, 1383–1396, doi:10.1139/X03-087.
Sutton, R. J., M. L. Deas, S. K. Tanaka, T. Soto, and R. A. Corum (2007), Salmonid observations at a Klamath River thermal refuge under various hydrological and meteorological conditions, *River Res. Appl.*, *23*(7), 775–785, doi:10.1002/rra.1026.
Tague, C., M. Farrell, G. Grant, S. Lewis, and S. Rey (2007), Hydrogeologic controls on summer stream temperatures in the McKenzie River basin, Oregon, *Hydrol. Processes*, *21*(24), 3288–3300, doi:10.1002/hyp.6538.
Taylor, C. A., and H. G. Stefan (2009), Shallow groundwater temperature response to climate change and urbanization, *J. Hydrol.*, *375*(3–4), 601–612, doi:10.1016/j.jhydrol.2009.07.009.
Taylor, R. G., et al. (2013), Groundwater and climate change, *Nat. Clim. Change*, *3*, 322–329, doi:10.1038/nclimate1744.
Teutschbein, C., and J. Seibert (2012), Bias correction of regional climate model simulations for hydrological climate-change impact studies: Review and evaluation of different methods, *J. Hydrol.*, *456–457*, 12–29, doi:10.1016/j.jhydrol.2012.05.052.
Torgersen, C. E., D. M. Price, H. W. Li, and B. A. McIntosh (1999), Multiscale thermal refugia and stream habitat associations of chinook salmon in northeastern Oregon, *Ecol. Appl.*, *9*(1), 301–319, doi:10.1890/1051-0761(1999)009[0301:MTRASH]2.0.CO;2.
Torgersen, C. E., J. L. Ebersole, and D. M. Keenan (2012), Primer for identifying cold-water refuges to protect and restore thermal diversity in riverine landscapes, *Rep. EPA 910-C-12-001*, *78* pp., U.S. Environ. Prot. Agency, Water Div., Seattle, Wash.
van Vliet, M. T. H., F. Ludwig, J. J. G. Zwolsman, G. P. Weedon, and P. Kabat (2011), Global river temperatures and sensitivity to atmospheric warming and changes in river flow, *Water Resour. Res.*, *47*, W02544, doi:10.1029/2010WR009198.
van Vliet, M. T. H., W. H. P. Franssen, J. R. Yearsley, F. Ludwig, I. Haddeland, D. P. Lettenmaier, and P. Kabat (2013), Global river discharge and water temperature under climate change, *Global Environ. Change*, *23*(2), 450–464, doi:10.1016/j.gloenvcha.2012.11.002.

Voss, C. I., and A. M. Provost (2002), SUTRA: A model for saturated-unsaturated variable-density ground-water flow with solute or energy transport, *Water Resour. Invest. Rep. 02–4231*, *201* pp., U.S. Geol. Surv., Reston, VA.

Watanabe, K., and T. Wake (2008), Hydraulic conductivity in frozen unsaturated soil, in *Proceedings of the 9th International Conference on Permafrost*, edited by D. L. Kane et al., pp. 1927–1932, Univ. of Alaska, Fairbanks, Alaska.

Webb, B. W., D. M. Hannah, R. D. Moore, L. E. Brown, and F. Nobilis (2008), Recent advances in stream and river temperature research, *Hydrol. Processes*, *22*(7), 902–918, doi:10.1002/hyp.6994.

Wilbur, N., and R. A. Curry (2011), Investigating and identifying thermal refugia for Atlantic salmon and brook trout in New Brunswick rivers using thermal infra-red technology, 11–01, New Brunswick Cooperative Fish and Wildlife Research Unit, Fredericton, NB, Canada.

Woo, M. (2012), *Permafrost Hydrology*, Springer, New York.

Woodbury, A. D., and L. Smith (1985), On the thermal effects of three-dimensional groundwater flow, *J. Geophys. Res.*, *90*(2), 759–767, doi: 10.1029/JB090iB01p00759.

Wu, H., J. S. Kimball, M. M. Elsner, N. Mantua, R. F. Adler, and J. Stanford (2012), Projected climate change impacts on the hydrology and temperature of Pacific Northwest rivers, *Water Resour. Res.*, *48*, W11530, doi:10.1029/2012WR012082.

Yin, X., and P. A. Arp (1993), Predicting forest soil temperature from monthly air temperature and precipitation records, *Can. J. For. Res.*, *23*(12), 2521–2536, doi:10.1139/x93-313.

Zhang, Y., S. K. Carey, and W. L. Quinton (2008), Evaluation of algorithms and parameterizations for ground thawing and freezing simulation in permafrost regions, *J. Geophys. Res.*, *113*, D17116, doi:10.1029/2007JD009343.